

TECHNICAL REPORT 83-24

**ACTINIDE SOLUBILITY IN DEEP
GROUNDWATERS – ESTIMATES FOR
UPPER LIMITS BASED ON CHEMICAL
EQUILIBRIUM CALCULATIONS**

M. SCHWEINGRUBER

DECEMBER 1983

**SWISS FEDERAL INSTITUTE FOR REACTOR RESEARCH
WÜRENLINGEN**

Nagra
Nationale
Genossenschaft
für die Lagerung
radioaktiver Abfälle

Cédra
Société coopérative
nationale
pour l'entreposage
de déchets radioactifs

Cisra
Società cooperativa
nazionale
per l'immagazzinamento
di scorie radioattive

TECHNICAL REPORT 83-24

**ACTINIDE SOLUBILITY IN DEEP
GROUNDWATERS – ESTIMATES FOR
UPPER LIMITS BASED ON CHEMICAL
EQUILIBRIUM CALCULATIONS**

M. SCHWEINGRUBER

DECEMBER 1983

SWISS FEDERAL INSTITUTE FOR REACTOR RESEARCH
WÜRENLINGEN

TABLE OF CONTENTS

Foreword	
Acknowledgements	
ABSTRACT / ZUSAMMENFASSUNG / RESUME	
1. INTRODUCTION	1
2. MODEL	3
2.1 Overview	3
2.2 Summary of theory	4
2.3 Computer code	4
2.4 Parameter selection	5
2.4.1 Temperature	5
2.4.2 pH	5
2.4.3 Eh	5
2.4.4 Thermodynamic database	7
2.4.5 Chemical composition of groundwater	11
2.4.6 Ionic strength	14
3. RESULTS	15
3.1 Thorium	15
3.1.1 Presentation	15
3.1.2 Validation	15
3.2 Uranium	18
3.2.1 Presentation	18
3.2.2 Validation	28
3.3 Neptunium	31
3.3.1 Presentation	31
3.3.2 Validation	38
3.4 Plutonium	41
3.4.1 Presentation	41
3.4.2 Validation	48
3.5 Americium	51
3.5.1 Presentation	51
3.5.2 Validation	52
4. SUMMARY AND CONCLUSIONS	54
5. REFERENCES	60
APPENDIX A : THERMODYNAMIC DATA	
APPENDIX B : MODEL DESCRIPTION	

Foreword

Part of the work on radioactive waste management performed at EIR Wuerenlingen is financially supported by NAGRA. This is the case for studies concerned with the modelling of geospheric nuclide transport. Hence, this document is issued simultaneously as EIR Report and NAGRA Technical report.

Acknowledgements

The author would like to thank A. Bundi, B. Goodwin, R. Grauer, J. Hadermann, I.G. McKinley and F.J. Pearson Jr. for encouragement, discussions and constructive criticism, H.P. Alder, H. Flury and Ch. McCombie for their interest, and NAGRA for partial financial support.

The technical assistance of I. Kusar and S. Wittke Jr. during the preparation of the report is appreciated.

C. Bajo was so kind to translate the abstract into French.

ABSTRACT

A chemical equilibrium model is used to estimate maximum upper concentration limits for some actinides (Th, U, Np, Pu, Am) in groundwaters. Eh/pH diagrams for solubility isopleths, dominant dissolved species and limiting solids are constructed for fixed parameter sets including temperature, thermodynamic database, ionic strength and total concentrations of most important inorganic ligands (carbonate, fluoride, phosphate, sulphate, chloride). In order to assess conservative conditions, a reference water is defined with high ligand content and ionic strength, but without competing cations. In addition, actinide oxides and hydroxides are the only solid phases considered.

Recommendations for 'safe' upper actinide solubility limits for deep groundwaters are derived from such diagrams, based on the predicted Eh/pH domain. The model results are validated as far as the scarce experimental data permit.

ZUSAMMENFASSUNG

Mit Hilfe eines chemischen Gleichgewichtsmodells werden Speziation und maximale Löslichkeitslimiten einiger Aktiniden (Th, U, Np, Pu, Am) in natürlichen Grundwässern abgeschätzt. Für festgelegte Parametersätze (Temperatur, thermodynamische Daten, Ionenstärke, Totalkonzentrationen wichtiger Liganden) werden Eh/pH-Diagramme mit Löslichkeitsisoplethen, dominierenden gelösten Spezies und limitierenden Festphasen konstruiert. Im Sinne einer konservativen Analyse wird ein Referenzwasser mit hohem Gehalten an anorganischen Liganden (Carbonat, Fluorid, Phosphat, Sulfat, Chlorid), mit hoher Ionenstärke, aber ohne konkurrierende Kationen eingeführt; zudem sind bloss Aktiniden-oxide und -hydroxide als limitierende Phasen zugelassen.

Aufgrund der wahrscheinlichen Eh/pH-Grenzen für tiefe Grundwässer werden Empfehlungen für 'sichere' Löslichkeitslimiten abgeleitet. Soweit dies die spärlichen experimentellen Befunde zulassen, werden die Ergebnisse auf ihre Konservativität überprüft.

RESUME

Les espèces chimiques et les limites de solubilité maximales de quelques actinides (Th, U, Np, Pu, Am) sont estimées, à l'aide d'un modèle d'équilibres chimiques, dans des eaux souterraines naturelles. Des diagrammes Eh/pH sur lesquels figurent les isoplètes de solubilité, les espèces chimiques dominantes dissoutes et les phases solides limitantes sont construits pour des ensembles de paramètres bien définis (température, données thermodynamiques, force ionique, concentration en ligands tels que carbonate, fluorure, phosphate, sulphate, chlorure). On a défini une eau de référence "conservatrice", riche en ligands inorganiques, de force ionique élevée, mais dépourvue de cations concurrents. Les seules phases solides considérées sont les oxydes et les hydroxydes d'actinides.

Des limites de solubilité "sûres" sont recommandées. Elles sont déduites des conditions Eh/pH vraisemblables pour les eaux souterraines. Pour autant que les rares constatations expérimentales le permettent, les résultats du modèle sont vérifiés en ce qui concerne leur conservatisme.

1. INTRODUCTION

The assessment of actinide solubilities under geospheric conditions is of considerable relevance to the safety analysis for projected radioactive waste repositories since, over geologic timescales, long-lived actinide isotopes represent the dominant potential hazard to the biosphere. These nuclides include both isotopes initially present in the waste (Np-237, Pu-239, Pu-240, Am-241, Am-243) and daughter products formed in the U-235, U-238 and Am-241/Np-237 decay chains (Pa-231, Th-230, Th-231) (Allard (1983)).

Information about concentration limits of such elements in groundwater and about their complexation pattern in solution can be obtained from theoretical models based on the premise of chemical equilibrium conditions. The results of such speciation and solubility calculations may be considered as first indicators to justify boundary conditions or parameter choices for mathematical models of nuclide transport in geosphere. This approach, however, remains tentative as long as the insignificance of kinetic effects, which imply non-equilibrium conditions, can not be demonstrated for the system in consideration.

Various reports concerned with the prediction of actinide solubility have been issued since the late 1970's. For example, the work of Rai and Serne (1978) includes a summary of equilibrium constants at 25 C for the entire spectrum of radwaste elements; their actinide database is, however, not very extensive, and their solubility calculations concentrate on aerated systems. Allard (1982, 1983) describes actinide solubilities in carbonate waters at 25 C and 1 atm. His thermodynamic datasets include extrapolated or estimated data for actinide species which are likely to exist but have not yet been experimentally identified (basic assumption : chemical similarity of single actinide oxidation states). His main variables are pH, carbon dioxide partial pressure and redox potential; the latter is either treated as independent variable or explicitly specified as function of pH. Activity/concentration conversions are neglected. Skytte Jensen (1982) constructed stability diagrams describing speciation as well as isoconcentration curves for the transuranium elements in the Eh/pH field. His study is, again, limited to hydroxide and carbonate species and does not account for ionic strength or temperature effects. Goodwin (1980, 1982) calculated maximum uranium solubilities for groundwater conditions representative for those expected for Canadian nuclear waste vaults. With the thermodynamic database for dissolved and solid uranium species given by Lemire and Tremaine (1980), he was able to depict the effects of pH, Eh, temperature and a more extensive groundwater chemistry under specific conditions. An analogous study was performed for potential solubility of U, Pu, Np and Th in two selected Swiss groundwaters (Schweingruber (1981, 1982a)).

The present report attempts to state "reasonably conservative" upper concentration limits for a series of actinides (Th, U, Np, Pu, Am) under typical deep groundwater conditions. It will include efforts to account for potential effects of elevated temperatures and ionic strengths as well as for actinide complex formation with additional inorganic ligands, such as fluoride, phosphate, sulphate and chloride.

The aspect of conservatism, in the sense of overestimation of effective solubility, is introduced as follows : first, we assume that only a subset of potential actinide solids, the oxides and hydroxides, can actually limit solubility. Second, we define a reference groundwater such that it (1) contains high but still realistic concentrations of inorganic anions (carbonate, phosphate, sulphate, fluoride, chloride) and (2) that it is free of additional cations which would compete with the actinide for complexation. Note that the degree of conservatism is, of course, a relative one since, for instance, neither organic ligands nor colloidal aggregates are included in the model. Hence, the importance of subsequent model validation must be emphasized.

Temperature, pH, Eh and thermodynamic database are the main model parameters. 'Non-ideal' solution behaviour is simulated by fixing ionic strength at a relatively high level. In general, a four-step procedure is foreseen for each element: (1) statement of maximum solubility, limiting solid and dominant dissolved species as a function of pH and Eh for given temperature and database; (2) statement of maximum solubility and speciation as a function of pH for three fixed Eh/pH-relationships representative of lower and upper Eh/pH boundaries for reducing groundwaters and of an oxygenated water; (3) comparison of model results obtained with different parameter sets; (4) check of model conservatism with respect to observations.

2. MODEL

2.1 Overview

The mathematical model outlined below was designed to estimate speciation (i.e. elemental distribution between various dissolved species) and maximum solubility of multivalent actinides in aqueous solution under the following premises :

(1) chemical equilibrium in solution among all components considered, including redox equilibria amongst various actinide oxidation states;

(2) actinide solubility exclusively limited by pure oxide or hydroxide solids;

(3) closed system for identified chemical constituents other than hydrogen ion, hydroxide ion and actinide aquo ions (i.e. carbonate, sulphate, fluoride, chloride, phosphate);

(4) simulation of temperature effects with a simple van't Hoff approach (assuming standard reaction enthalpies to be constant within the temperature intervals considered);

(5) activity coefficients for dissolved species approximated with Davies' formula;

(6) neglect of pressure effects.

The key parameters include :

(i) temperature (T);

(ii) pH;

(iii) redox potential (Eh);

(iv) ionic strength (I);

(v) total concentrations for all components except hydrogen ion, hydroxide ion and actinide aquo ions;

(vi) stoichiometric and thermodynamic descriptors for all pertinent reactions, collected in databases (db).

Section 2.2 summarizes the theoretical background and a short reference to the adopted computer codes is given in Section 2.3. The selection of parameter values or ranges is discussed in Section 2.4.

2.2 Summary of theory

This section is intended to point out the fundamental structure of the model based on the premises listed in the previous section. For a more detailed analysis, the reader is referred to Appendix B.

The subsequent logical steps may be sketched as :

(i) - establishment of an equilibrium constant database including pertinent dissolved species, solids and redox equilibria for given temperature and ionic strength, based on assumptions (4), (5) and (6).

(ii) - definition of upper activity (or concentration) limits for actinide aquo ions and of the solubility-limiting solid for fixed pH and Eh, based on premises (1) and (2).

(iii) - solution of the mass balance equation system for the residual chemical components under the constraints of fixed pH, Eh and actinide aquo ion concentrations (assumption (3)).

(iv) calculation of maximum actinide solubility and actinide speciation.

2.3 Computer code

The model concept presented in Section 2.2 is compatible with the logic of the speciation program MINEQL (Westall et al. (1976), Schweingruber (1981)). MINEQL calculates the equilibrium composition of aqueous solutions using the equilibrium constant method: the set of component mass balances is iteratively solved with a Newton-Raphson algorithm. Solid/solution, gas/solution and redox equilibria are accepted as boundary conditions.

The original MINEQL subroutine package has been extended at EIR; it now includes programs for an automatic temperature conversion of equilibrium constants and for representation of activity coefficients (Schweingruber (1982b)).

Two programs based on MINEQL have been designed for the present purpose. The first one (internal name MAIN27) computes actinide solubility and speciation for independent Eh/pH variation (fixed grid), the second (MAIN26) uses a fixed Eh/pH-relationship (pH range and stepwidth fixed). Both programs search for the limiting solid by a trial and error method and are linked to plot programs for convenient presentation of results.

2.4 Parameter selection

2.4.1 Temperature

Ambient temperatures are in the order of 50 to 75 C for granitic rock formations envisaged as hosts for high-level waste in current Swiss waste management concepts. Depending on repository design, waste treatment, time and other factors, vault temperatures can be expected to range between 60 and more than 100 C at any point in time (NAGRA (1980)). A temperature interval of 10 to 100 C seems to be appropriate for the far-field extending to the biosphere.

Most of the calculations presented below will be for 25 C only. One reason is the large uncertainty already connected with equilibrium constants for 25 C. In addition, the enthalpy data required to establish high-temperature log K databases (Section 2.2.3) are frequently not at hand. Tentative calculations will be performed for 75 C, however, when justified by database quality.

2.4.2 pH

pH will be considered as a variable ranging between 5.5 and 10. These limits bracket most pH values reported for groundwaters (see e.g. Table 3). Deep granitic waters are generally neutral to slightly basic (pH 7 to 9).

2.4.3 Eh

Like pH, Eh will be treated as an independent variable. Its lower and upper boundary values (-400 mV and +700 mV, respectively) have been fixed such that the entire probable Eh/pH domain for groundwaters is covered for pH range 5.5 to 10 (Fig. 1). This strategy will allow analysis of the sensitivity of actinide solubility with respect to Eh. Possible uses of such a procedure include evaluation of the effect of Eh changes in the geologic environment (e.g. an Eh increase due to radiolysis within a repository) and estimation of maximum actinide solubilities within limited Eh/pH fields.

In Fig. 1, Sato (1960) distinguishes between Eh/pH domains for oxygen-depleted deep groundwaters and for aerated waters. In the present analysis we utilize his lower and upper boundaries for the depth environment, which are thought to bracket Eh/pH conditions in undisturbed deep granite formations, and a rather arbitrary function representative for a 'weathering' environment.

Figure 1: Probable Eh/pH domains in groundwaters (Sato (1960)).
Line numbers denote Eh/pH relationships referred to in Table 1.

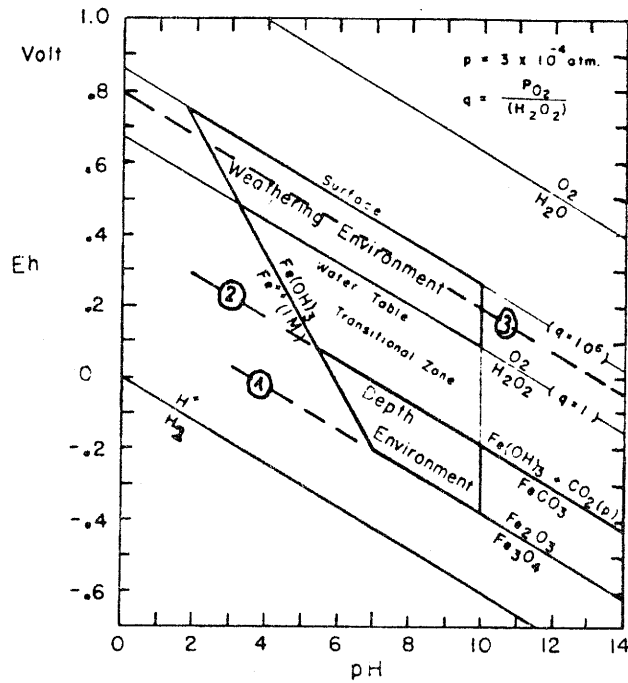


Table 1: Analytical definition of selected Eh/pH relationships.
Function is $Eh[mV] = E0 - 59 pH$.

assignment	line number	$E0[SHE, mV]$
low Eh limit, deep groundwater	(1)	220 a
high Eh limit, deep groundwater	(2)	407 b
typical Eh, weathering environment	(3)	800 c

a interpretable in terms of hematite/magnetite equilibrium,
 $3/2 Fe_2O_3 + (H^+) + (e^-) = Fe_3O_4 + 1/2 H_2O$,
 at 25 C, 1 atm (Sato (1960)).

b interpretable in terms of ferric hydroxide/siderite eql.,
 $Fe(OH)_3 + CO_2(g) + (H^+) + (e^-) = FeCO_3 + 2 H_2O$,
 at 25 C, 1 atm, $\log pCO_2 = -3.5$ (Sato (1960)).

c proposed by Allard (1982).

The corresponding functions are defined in Table 1 (similar or identical fixed Eh/pH relationships have also been used by Goodwin (1982) and Allard (1981, 1983)). The empirical Eh limits for the reduced groundwaters will be taken as defined in Table 1 for model validation and for prediction of maximum actinide solubilities in deep granitic waters. This approach is, of course, tentative in that the Eh/pH domain for such waters would depend on temperature and CO₂ partial pressure if the chemical interpretation of the boundary lines is correct (see footnotes in Table 1).

The validity of the the lower Eh/pH boundary for reducing groundwaters is supported by Eh/pH couples reported for Swiss well waters (NAGRA (1981)): the observed potentials all lie above theoretical values obtained for an assumed hematite/magnetite equilibrium (Schweingruber (1983)). Sato's Eh/pH domain for deep groundwaters is compatible with data Allard (1983) cited for borehole waters from Swedish granites.

2.4.4 Thermodynamic database

As summarized by Table 2, actinides are present in nature in a variety of oxidation states as a consequence of their particular electron configuration. Typically, the most stable valency under oxidizing conditions first increases with increasing atomic number (from +III for Ac to +VI for U) and then decreases to +III for the higher actinides. Lower oxidation states may, however, become important in aqueous solutions under reducing conditions. Indeed, several oxidation states of an actinide (especially Np, Pu) can coexist in comparable concentrations. In this study we will consider the following valencies: Th(IV), U(III,IV,V,VI), Np(III,IV,V,VI), Pu(III,IV,V,VI), Am(III).

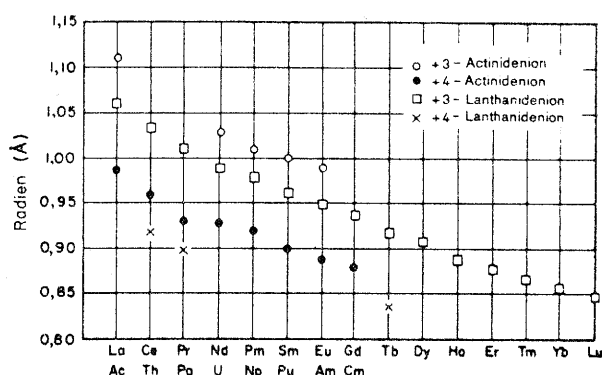
The aquo ions of the oxidation states III to VI can be described as M⁺³, M⁺⁴, MO₂⁺, and MO₂⁺², respectively (Cotton and Wilkinson (1970)). These ions are generally classified as 'hard': they form strong complexes with 'hard' ligands such as fluoride and oxygen-donors (e.g. hydroxide, carbonate, phosphate, sulphate (less important)) but show little affinity to 'soft' ligands (sulfide, iodide, bromide). Complex formation is usually dominated by electrostatic effects. The charge effect can be stated as M⁺⁴ > MO₂⁺² > M⁺³ > MO₂⁺, and the ionic radii of identical valencies decrease with increasing atomic number (actinide contraction, Fig. 2). This effect as well as the similarity of comparable lanthanide and actinide aquo ion radii is frequently used to predict thermodynamic properties of actinide species (e.g. Baes and Mesmer (1976), Allard (1982)).

Table 2 : Detected actinide oxidation states (Cotton and Wilkinson (1970)).

Ac	Th	Pa	U	Np	Pu	Am	Cm	Bk	Cf	Es	Fm	Md
3 ^a	3 ^b	3	3	3	3	3	3	3	3	3	3	3
	<i>4</i>	4	4	4	4	4	4	4				
		<i>5</i>	5	5	5	5						
			<i>6</i>	6	6	6						

a italics : most stable valencies under atmospheric condition
 b only in solid state

Figure 2: Radii of actinide and lanthanide aquo ions (Cotton and Wilkinson (1970)).



Experimental determination of thermochemical data for aqueous species and solids is very difficult due to the extreme complexity of actinide chemistry, requiring rigorous control of experimental conditions (e.g. redox potential, CO₂ pressure, crystallinity of solids) and, frequently, very sensitive analytical techniques (measurements in cases of low solubilities). The use of isotopes with short half-lives may induce further complications such as radiation damage and radiolytic effects. Problems of this kind certainly contribute to the existence of large discrepancies in literature data. As an example, Figure 3 illustrates the large scatter for reported solubility products of tetravalent actinide oxides.

In view of these uncertainties, it was decided to operate the model with two alternative datasets which are displayed and assessed in Appendix A:

Database A (abbreviated as : db=A) is derived from recent compilations by Lemire and Tremaine (1980;U,Pu), Langmuir and Herman (1980;Th) and Phillips (1982;Am). It has been used previously at EIR (Schweingruber (1981,1982a)).

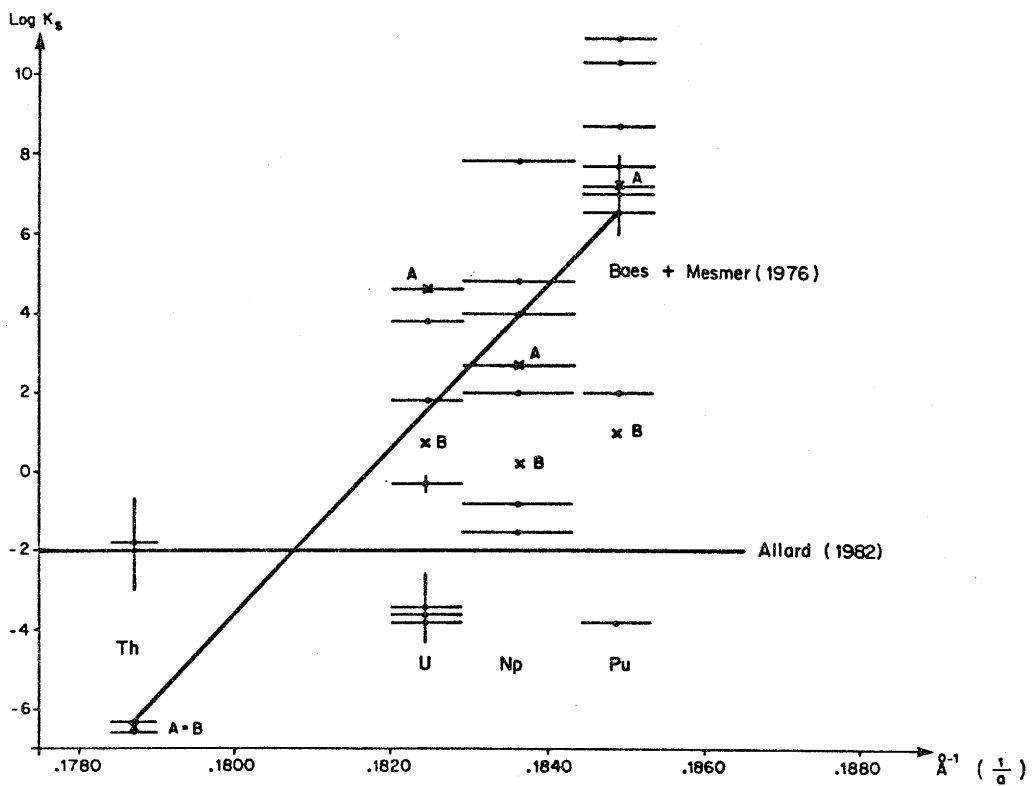
Database B (db=B) exclusively comprises the most recent data of Allard (1983).

Both datasets account for actinide hydrolysis and complex formation with carbonate, fluoride, phosphate, sulphate and chloride. Data on hydroxide and oxide solids and, for comparative purposes, on carbonate, fluoride and phosphate solids are also incorporated.

We may anticipate that the tetravalent actinide oxides will play an important role in determining solubility over a large Eh/pH domain. Figure 3 shows that the pertinent solubility products selected in database A scatter around the correlation proposed by Baes and Mesmer (1976) to extrapolate the stability of (isostructural) actinide(IV) oxides from their lattice parameter. The corresponding solubility products of database B are generally lower (2 to 6 orders of magnitude, except for Th where identical constants are used). Note the difference between the solubility products Allard defined in his general (1982) and more specific (1983, B points) databases, respectively.

Organic ligands are omitted in the present model. Tentative speciation calculations for Am(III) and Pu(IV) suggest that humate complexes could indeed affect their solubility under pH conditions and humic acid concentrations believed to be representative of deep groundwaters (Olofsson (1983)). The thermodynamic characterization of such complexes is difficult, however, due to the fact that humic or fulvic acids are not single compounds but a variety of macromolecules with operationally defined molecular weight intervals and similar chemical properties.

Figure 3: Variation of literature data on solubility products (K_s) of tetravalent actinide oxides based on reaction $(M+4) + 2 (H_2O) = MO_2(s) + 4 (H^+)$ and shown as a function of the reciprocal of the lattice parameter a (McKinley (1983a)). Horizontal bars for literature data denote uncertainties associated with the lattice parameter. Lines are model solubility constant functions given by Allard (1982) and Baes and Mesmer (1976). Crosses depict values integrated in databases A and B, respectively.



2.4.5 Chemical composition of the groundwater

Some analytical data for total concentrations of components pertinent to the thermodynamic database of the last section are listed in Table 3.

The concentration ranges for Swedish granite waters are, as expected, smaller than those of the regional NAGRA programme where data have been collected for waters originating in different geologic formations (including areas in the vicinity of salt and gypsum layers). The thermal wells of Zurzach and Saeckingen are included in this spectrum; they are explicitly listed because Zurzach water composition was selected for a previous actinide solubility study (Schweingruber (1981, 1982a)) and because the more saline Saeckingen water was taken as standard for experimental work on actinide/rock interaction at EIR (Bischoff (1982)).

For the sake of conservatism with respect to effective actinide solubility, the reference water for the present study was designed to have total ligand concentrations around the upper limits reported (with rounding-off adjustments for molar units, see Table 3).

Total carbonate concentration was modelled as a function of pH for a constant alkalinity ([Alk]) and ionic strength (I) as given in Table 3 :

$$[\Sigma \text{CO}_3] = [\text{Alk}] * g(\text{pH}) / h(\text{pH})$$

with

$$g(\text{pH}) = 3.45 + 2.91\text{E}10 * 10^{-\text{pH}} + 4.79\text{E}16 * 10^{-2\text{pH}}$$

and

$$h(\text{pH}) = 6.90 + 2.91\text{E}10 * 10^{-\text{pH}} .$$

This relationship was derived on the assumption of chemical equilibrium in a simplified carbonate system at 25 C and ionic strength 0.2, considering only carbonate, bicarbonate and dissolved CO₂. It is based (a) on the carbonate mass balance, (b) on mass action laws coupling pH and carbonate species (see Appendix A, Table A-2), (c) on a simplified analytical interpretation of the alkalinity and (d) on a modelling of species activity coefficients with Davies' approximation (see Appendix B, Table B-1).

Table 3 . Values or ranges for selected physico-chemical parameters in a few
 ----- groundwaters.

	unit	Saeckingen Badquelle	Zurzach well 1	NAGRA reg. programme	deep granite groundwater	reference water \$
main reference		a	a	a	b	-
Temperature	C	29	38	5-50	---	25,(75)
Ionic strength	-	.06@	.017@	.001-.25@	---	.2
pH	-	6.5	7.9	5.8-9.	7-9	5-10
Eh *	mV	400	180	-130/+500	---	-400/+700
Alkalinity	meq/l	4.8	4.2	.4-20.	1.5-7.	10
chloride	mg/l	1600	140	2-2000	4-15	1770#
fluoride	mg/l	3	10	.1-10	.5-5	19#
sulphate	mg/l	120	250	3-1500	.5-15	960#
phosphate	ug/l	70	50	8-300	10-200	490#

a NAGRA (1981)
 b Allard (1983)

@ estimated as not explicitly reported

* potential versus standard hydrogen electrode (SHE)

total concentrations set equal to 50 mM (Cl-), 1 mM (F-), 10 mM (SO4-2), .005 mM (PO4-3).

\$ used for modelling in present paper

Figure 4: Total carbonate concentration. Comparison of modelling for reference water (thick line) and gas extraction data for some natural or drilled well waters in northern Switzerland (triangles, NAGRA (1981)).

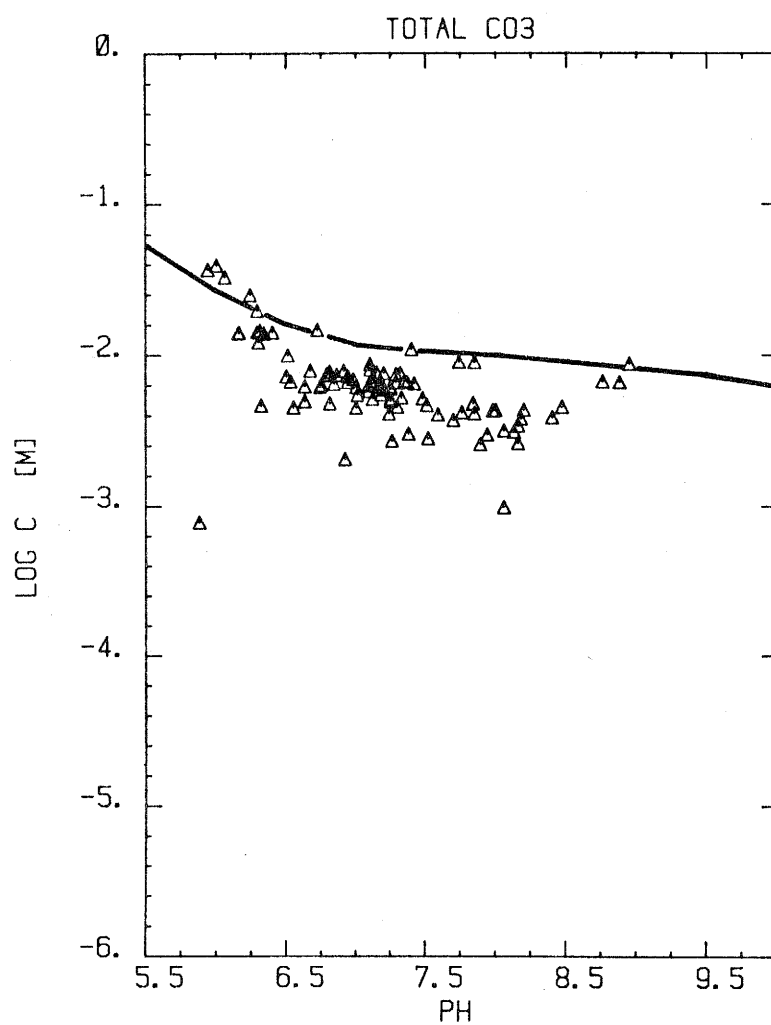


Fig. 4 shows that this function yields a reasonable upper envelope for actual total carbonate contents in a variety of Swiss groundwaters.

2.4.6 Ionic strength

Ionic strength was taken as a constant. Its value was fixed either as 0.2 (simulating realistic conditions in a rather conservative sense) or as 0 (omission of ionic strength effects in comparative runs).

Subsequent to every calculation with I equal 0.2, it was checked whether the modelled system could be realized within this ionic strength. Minimum values for effective ionic strength were computed by summation of the contributions of the identified species, adding a minimal contribution of non-identified species necessary to satisfy the condition of electroneutrality in solution. Typical values for minimum effective ionic strength are, with the model parameters from Table 3 and for low to moderate actinide solubilities, 0.1 for a single-charged and 0.15 for a double-charged counter-ion.

No speciation or solubility results are given, if the minimum ionic strength turned out to exceed the value of 0.2 (e.g. for Am at lower pH values, see Fig. 18).

3. RESULTS

3.1 Thorium

3.1.1 Presentation

Maximum Thorium solubility and its speciation in the reference water (Table 3) has been evaluated for three conditions:

(i) thermodynamic database A (mainly Langmuir and Herman (1980)) at 25 C;

(ii) database A at 75 C;

(iii) database B (Allard (1982,1983)) at 25 C.

The plots of Fig. 5 depict maximum solubility (S) and relative speciation (concentration C divided by solubility, only most important species denoted); they are valid for any of the Eh/pH relationships (1) to (3) defined in Table 1 since both datasets only include Th(IV) species.

At 25 C, both databases yield a fairly similar pH-dependency of the solubility. Since the solubility product of ThO₂(s) is the same in both cases (see Appendix A, Table A-5), the small differences must be attributed to variations in the data for dissolved species. The corresponding speciation plots illustrate that database B includes more stable fluoride and less stable phosphate complexes than base A.

With database A, a temperature increase from 25 to 75 C reduces solubility for pH < 8.5; the model predicts a minute temperature effect for pH > 8.5.

3.1.2 Validation

Langmuir and Herman (1980) noted that measured dissolved thorium in fresh surface waters (pH interval 5 - 8) usually range between 0.01 and 1 ppb. Filtrates of waters from the Morro del Ferro region in Brasil are reported to contain between (0.009+-0.004) and (0.12+-0.03) ppb Th (Eisenbud et al. (1982)). The pH is reported to vary between 4.4 and 7.2 in the stream with the highest dissolved Th content. Th concentrations observed in granitic waters from Fjallveden, Sweden, are also below or at the conservative limits predicted by any of the three solubility curves drawn in Fig. 5.

The curve for database A at 25 C is, provisionally, proposed to represent upper thorium concentration limits for deep groundwaters.

Figure 5: Solubility and speciation of Th in reference water. Dependency on pH, temperature (T) and database (db).

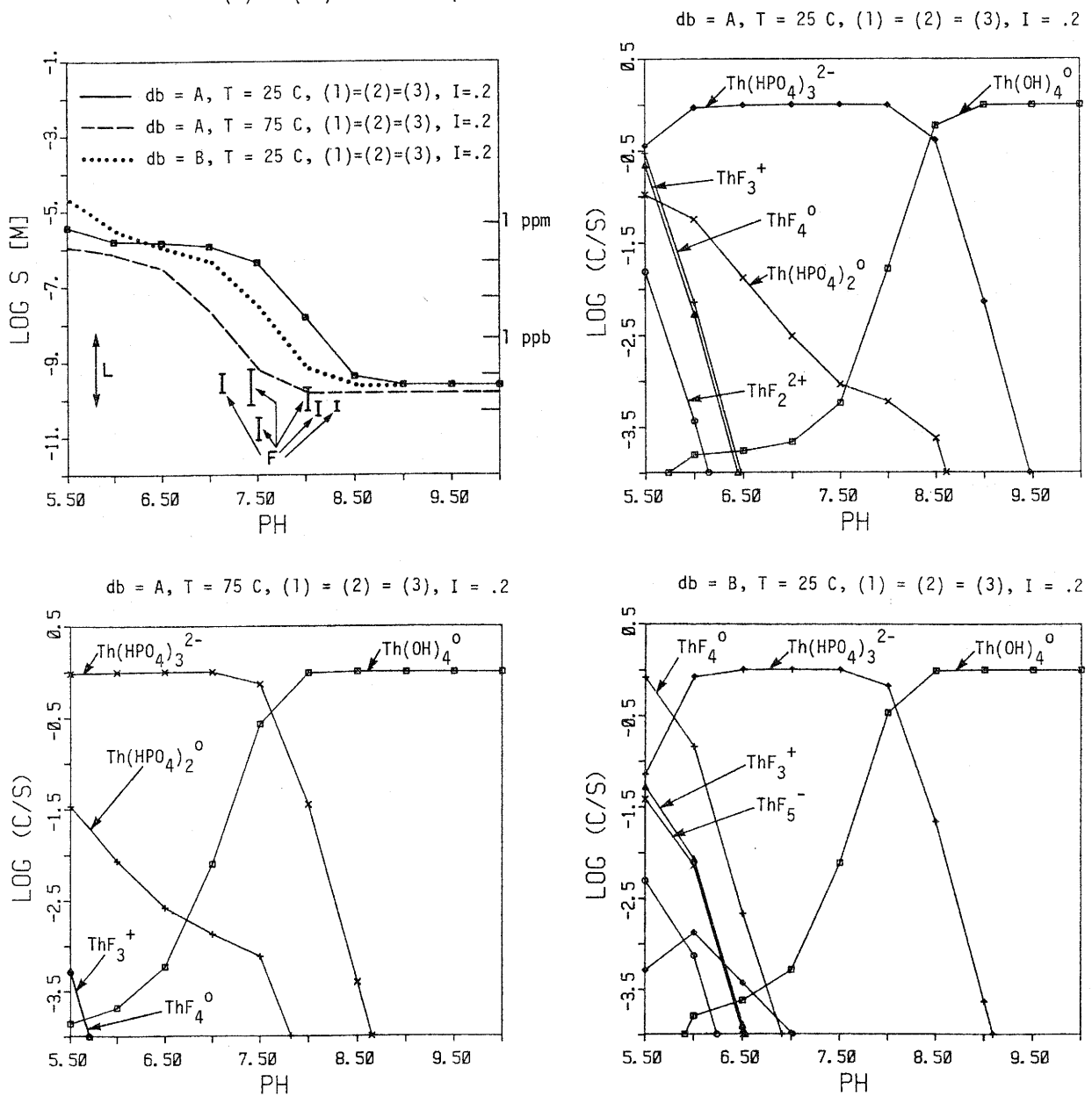
Experimental data points or ranges: L - typical groundwater values (Langmuir and Herman (1980)); F - Fjaellveden borehole samples (Laurent (1983)).

Th

Limiting solid : $\text{ThO}_{2(s)}$

Eh/pH functions :

- (1) Eh(mV) = 220 - 59 pH
- (2) Eh(mV) = 407 - 59 pH
- (3) Eh(mV) = 800 - 59 pH



3.2 Uranium

3.2.1 Presentation

Four case studies will be discussed with parameter selections and results summarized in Figs. 6 to 9.

Features common to all case studies are best seen by comparison of individual subfigures for each of the cases:

(a) - the oxidation states of the solubility limiting phases tend to change from +IV to +VI (with intermediates in Figs. 5 and 6) with increasing Eh and pH; UO₂ and U₄O₉ are the limiting solids within the reducing environment (bracketed by lines (1) and (2)).

(b) - the oxidation states of the dominant dissolved species behave similarly. Dissolved U(+VI) species may, however, already dominate in Eh/pH areas where UO₂ or U₄O₉ determines solubility. U(VI) carbonate complexes turn out to be most important, not only under oxidizing but also under reducing groundwater conditions, as soon as the free carbonate level is sufficiently high (pH > 6.5). Hydrolysis products of U(IV) as well as phosphate and fluoride complexes of U(VI) dominate in the residual Eh/pH field.

(c) - the solubility isopleths reveal a plateau under oxidizing conditions (Eh > 300 mV), leading to fairly pH-insensitive solubility curves for Eh/pH relation (3), varying in the order of .001 to .01 M. At very low potentials (Eh < -300 mV) the solubilities are low but noticeably increasing with increasing pH. Usually, a large solubility versus Eh gradient is observed within and around the Eh/pH field attributed to deep groundwaters suggesting that the definition of the upper limit, line (2), is of particular importance for the statement of maximum uranium solubilities expected for such conditions.

(d) - for a given pH, the solubility variation within the limits attributed to the reducing groundwaters (lines (1) and (2)) is generally larger than between the upper limit for the reducing environment (line (2)) and the reference line for oxidizing conditions (line (3)).

(e) - sulphate and chloride complexes are negligible since they never contribute above a 1% level to uranium solubility under all Eh/pH conditions considered.

The temperature effect is demonstrated by comparing subfigures (d) of Figs. 6 and 7. The shapes of curves (1) to (3) are not very different, but the solubilities in reducing environment increase by one or two orders of magnitude when going from 25 to 75 C. Also, carbonate complexes become more important at higher temperatures (subfigures (e)).

Figures 6 to 9. Uranium solubility and speciation in reference water.

Following cases are considered :

figure	database	temperature	ionic strength
-----	-----	-----	-----
6	A	25 C	0.2
7	A	75 C	0.2
8	B	25 C	0.2
9	B	25 C	0.

Following plots are shown in one figure :

(i) as a function of pH and Eh :

- (a) solubility limiting phase
- (b) dominant dissolved species
- (c) solubility isopleths (log. units; star denotes minimum, triangle maximum value)

(ii) as a function of pH :

- (d) solubility S
- (e) speciation (species concentration / solubility; only species above 1 % level specified)

for three selected Eh/pH relationships :

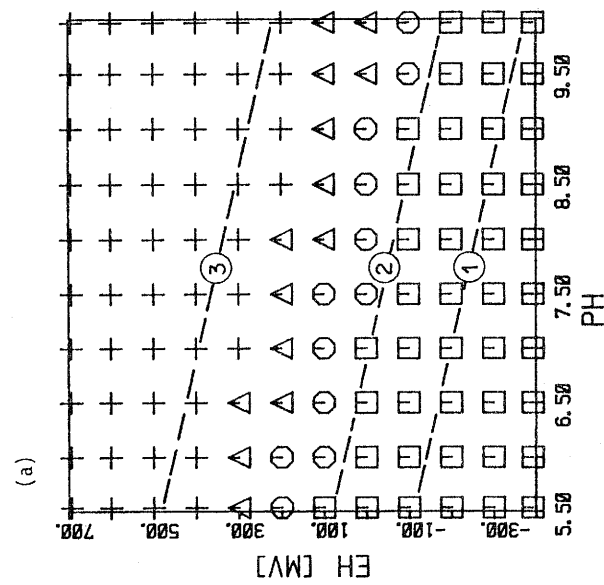
- (1) Eh[mV] = 220 - 59 pH
- (2) Eh[mV] = 407 - 59 pH
- (3) Eh[mV] = 800 - 59 pH

Figure 6

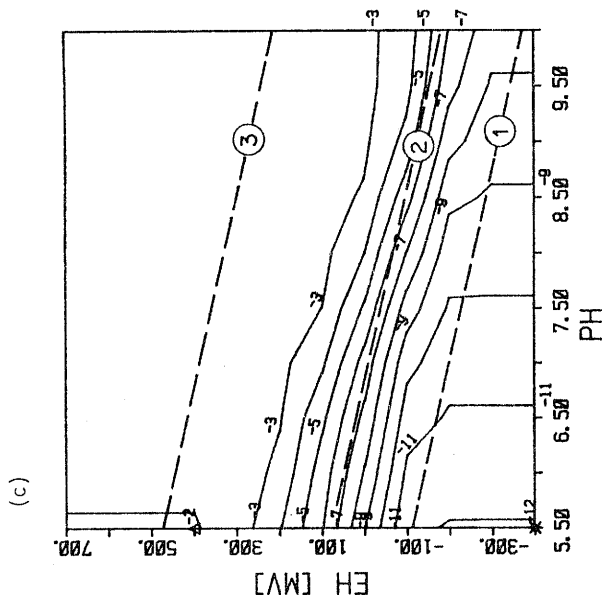
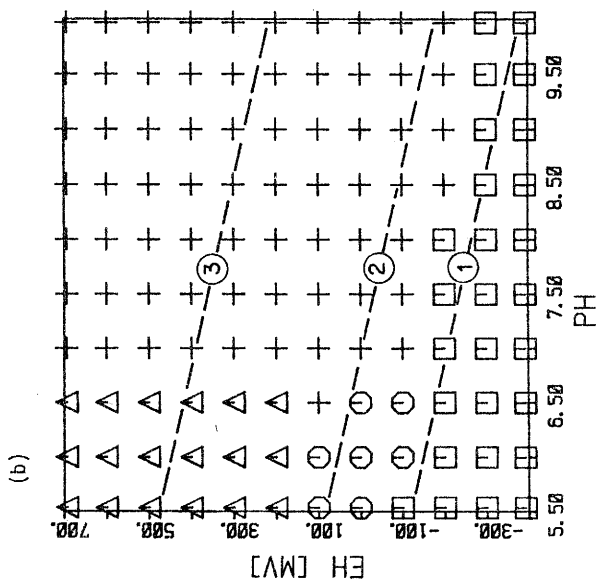
db = A, T = 25 C, I = 0.2

U

- \square UO_2 (s)
- \circ U_4O_9 (s)
- Δ U_3O_8 (s)
- $+$ $UO_2(OH)_2$ (s)



- \square $U(OH)_5^-$
- \circ $UO_2(HP0_4)_2^{2-}$
- Δ $UO_2(CO_3)_2^{2-}$
- $+$ $UO_2(CO_3)_3^{4-}$



- Eh/pH functions :
- (1) Eh(mV) = 220 - 59 pH
 - (2) Eh(mV) = 407 - 59 pH
 - (3) Eh(mV) = 800 - 59 pH

db = A, T = 25 C, I = 0.2

U

Eh/pH functions :

- (1) Eh(mV) = 220 - 59 pH
- (2) Eh(mV) = 407 - 59 pH
- (3) Eh(mV) = 800 - 59 pH

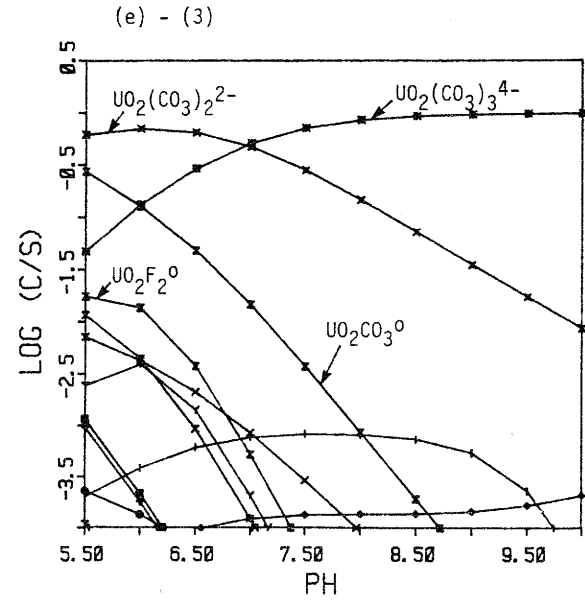
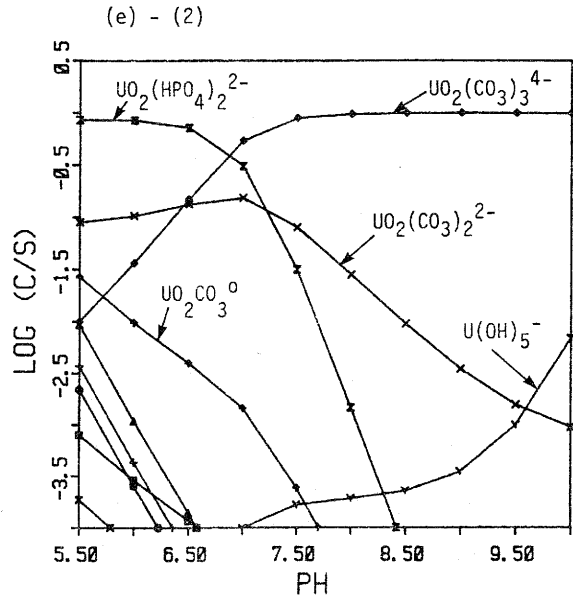
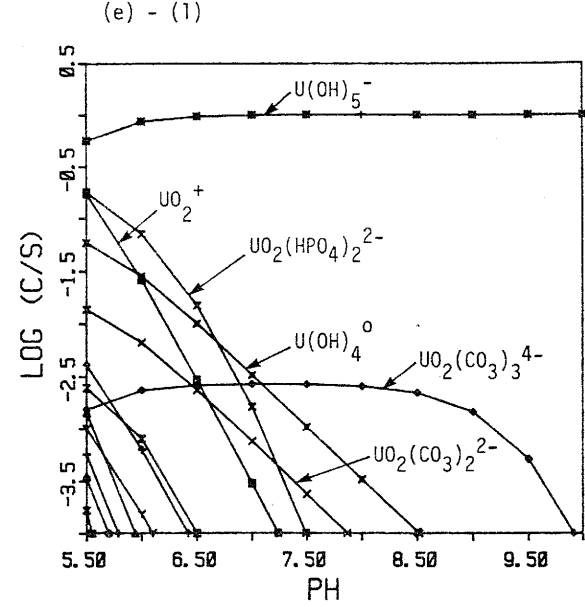
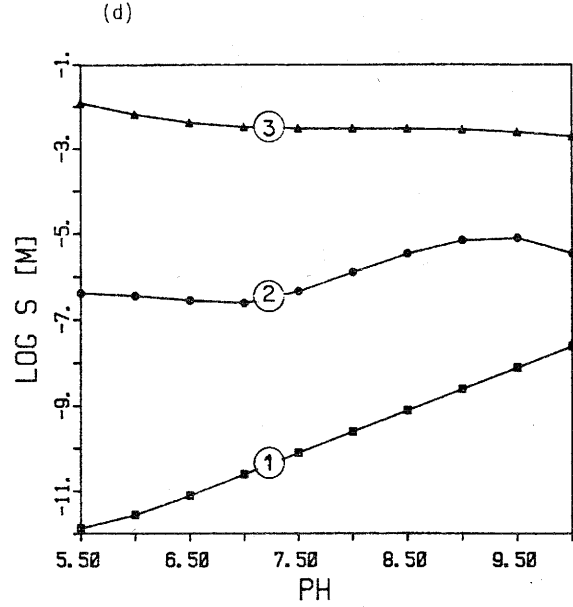
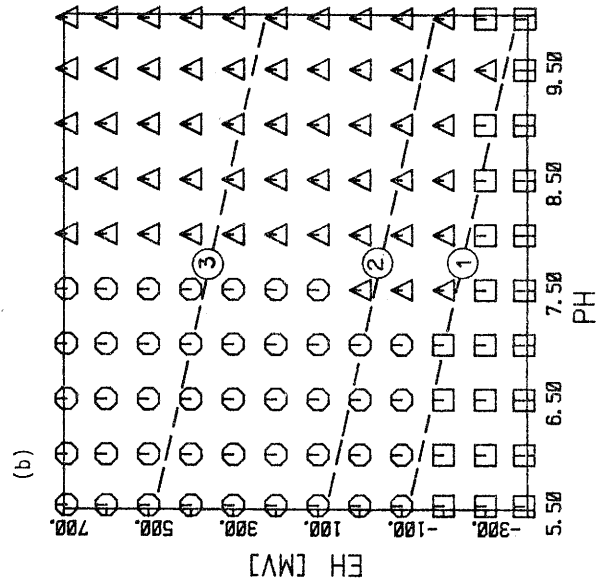
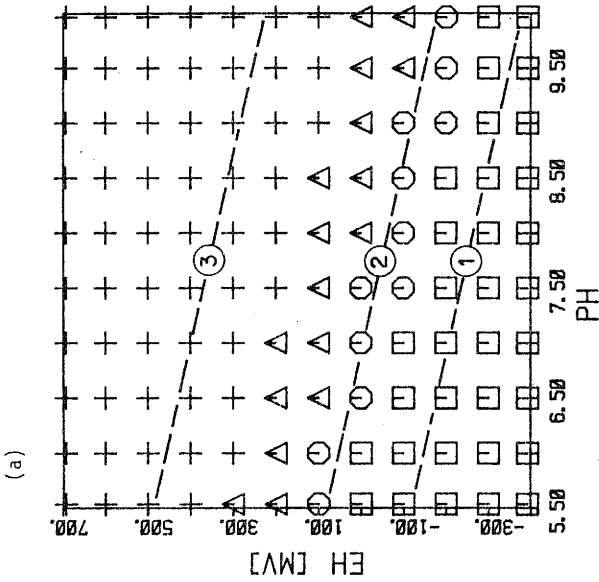


Figure 7

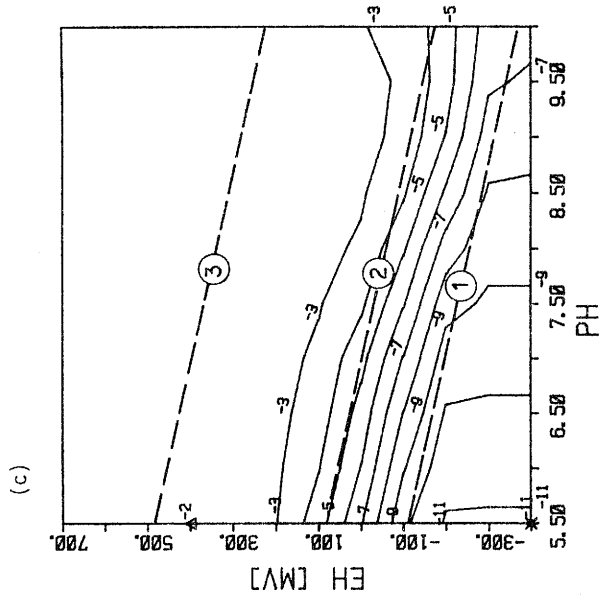
db = A, T = 75 C, I = 0.2

U

- UO_2 (s)
- U_4O_9 (s)
- △ U_3O_8 (s)
- + $UO_2(OH)_2$ (s)



- $U(OH)_5^-$
- $UO_2(CO_3)_2^{2-}$
- △ $UO_2(CO_3)_3^{4-}$



Eh/pH functions :

- (1) Eh(mV) = 220 - 59 pH
- (2) Eh(mV) = 407 - 59 pH
- (3) Eh(mV) = 800 - 59 pH

db = A, T = 75 C, I = 0.2

U

Eh/pH functions :

- (1) Eh(mV) = 220 - 59 pH
- (2) Eh(mV) = 407 - 59 pH
- (3) Eh(mV) = 800 - 59 pH

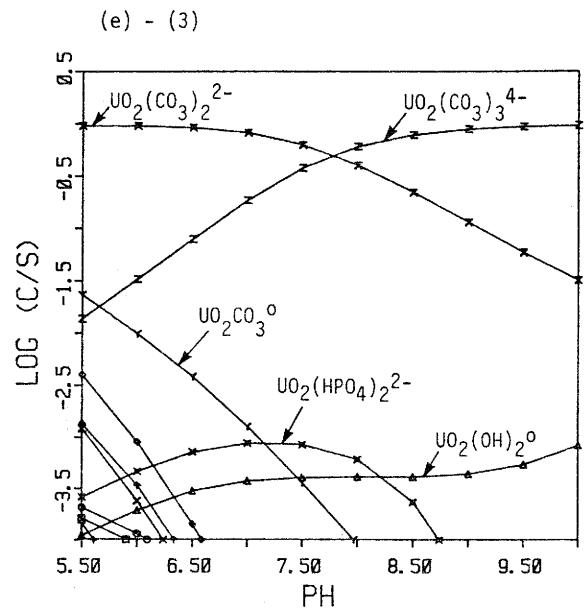
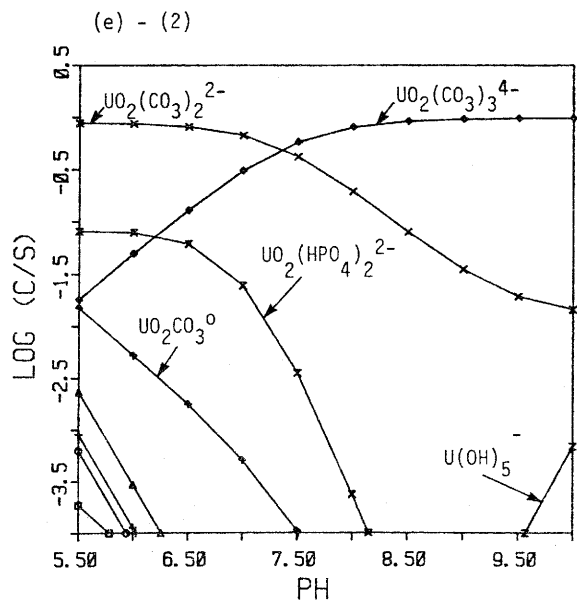
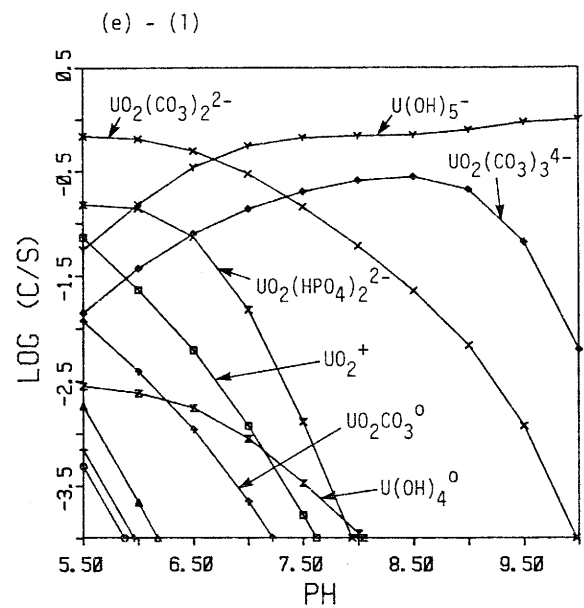
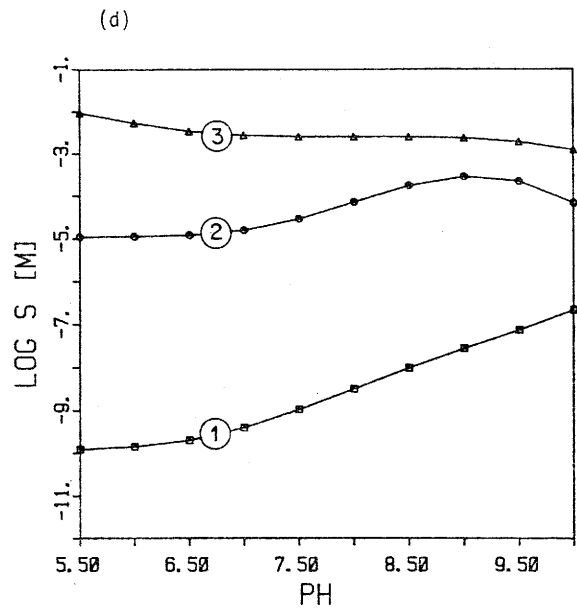
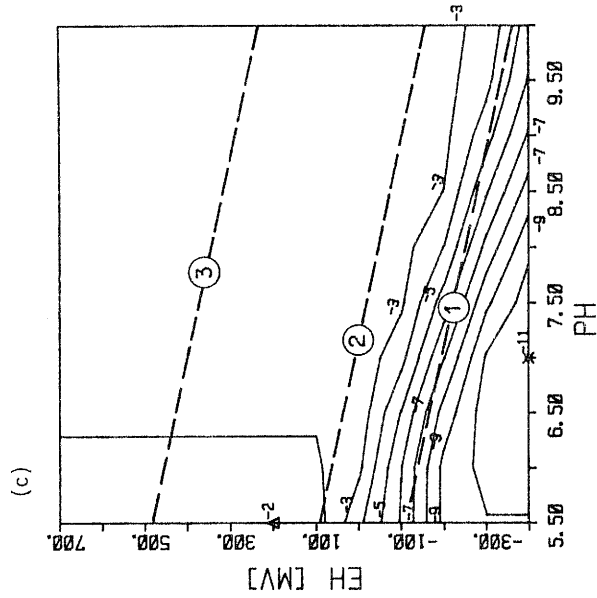


Figure 8

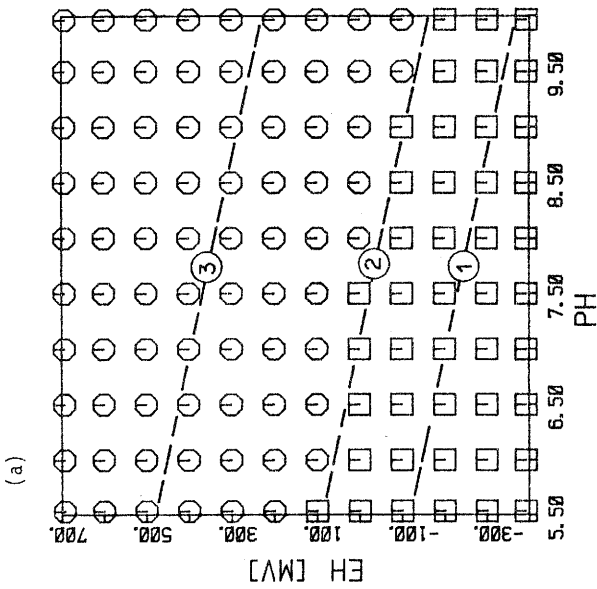
db = 8, T = 25 C, I = 0.2

U

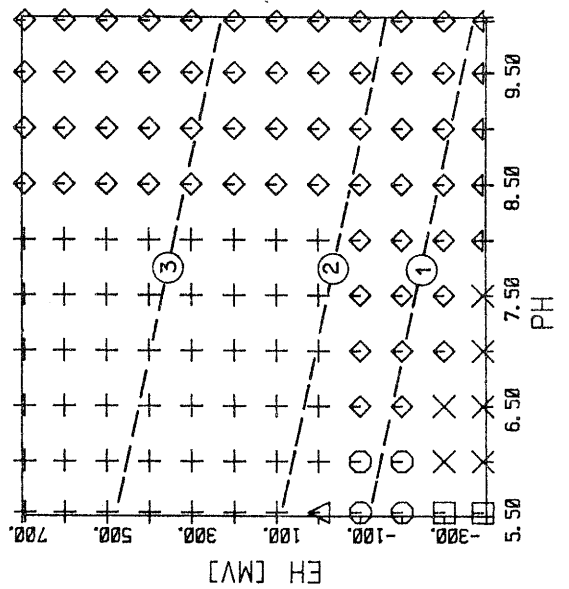


Eh/pH functions :

- (1) Eh(mV) = 220 - 59 pH
- (2) Eh(mV) = 407 - 59 pH
- (3) Eh(mV) = 800 - 59 pH



- UO₂ (s)
- UO₂(OH)₂ (s)



- U(HPO₄)₃²⁻
- UO₂F₄²⁻
- △ UO₂F₃⁻
- + (UO₂)₃(CO₃)₆⁶⁻
- × U(OH)₄⁰
- ◇ UO₂(CO₃)₃⁴⁻
- ⋈ UO₂(CO₃)₃⁵⁻

U

db = B, T = 25 C, I = 0.2

Eh/pH functions :

(1) Eh(mV) = 220 - 59 pH

(2) Eh(mV) = 407 - 59 pH

(3) Eh(mV) = 800 - 59 pH

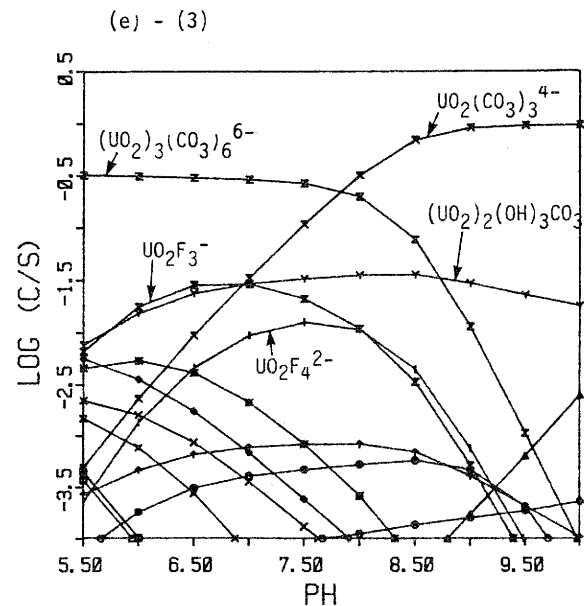
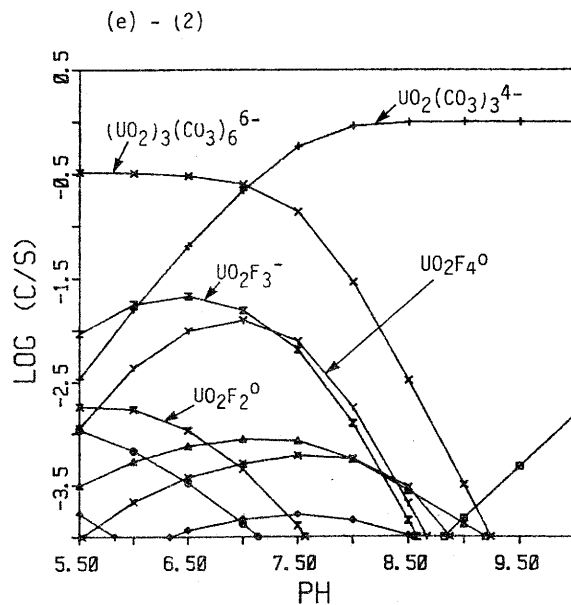
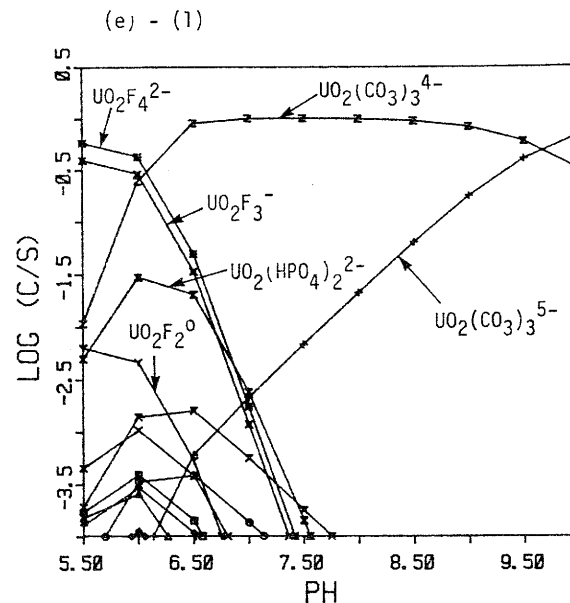
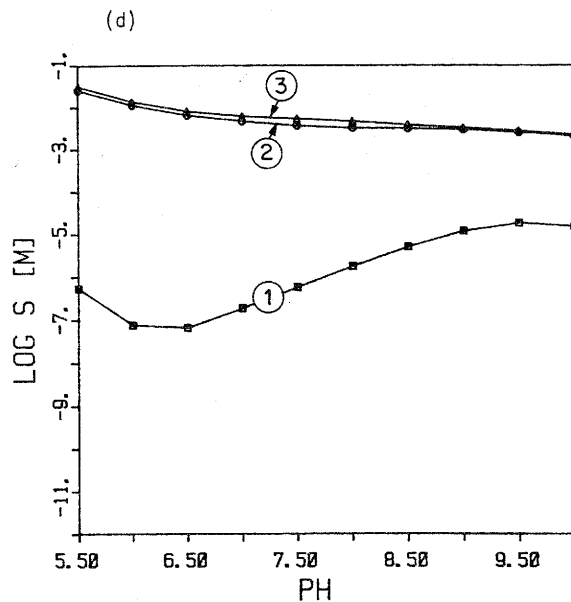
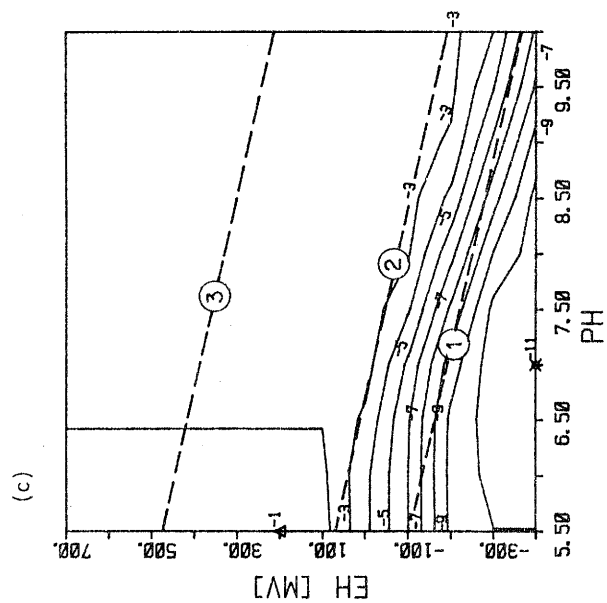


Figure 8 (continued)

Figure 9

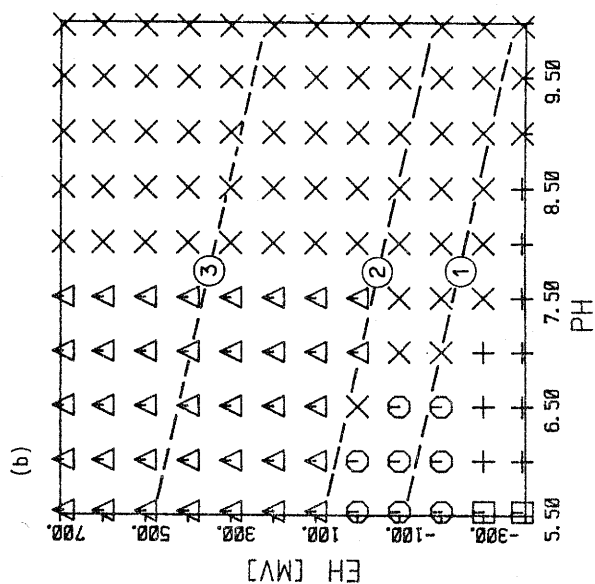
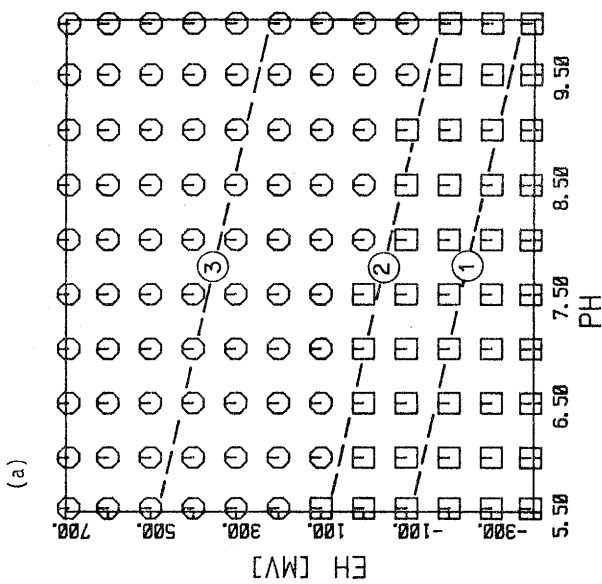
db = B, T = 25 C, I = 0

U



Eh/pH functions :

- (1) Eh(mV) = 220 - 59 pH
- (2) Eh(mV) = 407 - 59 pH
- (3) Eh(mV) = 800 - 59 pH



- UO_2 (s)
- $UO_2(OH)_2$ (s)

- $U(HPO_4)_3^{2-}$
- $UO_2F_3^-$
- Δ $(UO_2)_3(CO_3)_6^{6-}$
- + $U(OH)_4^0$
- X $UO_2(CO_3)_3^{4-}$

db = B, T = 25 C, I = 0

U

Eh/pH functions :

- (1) Eh(mV) = 220 - 59 pH
- (2) Eh(mV) = 407 - 59 pH
- (3) Eh(mV) = 800 - 59 pH

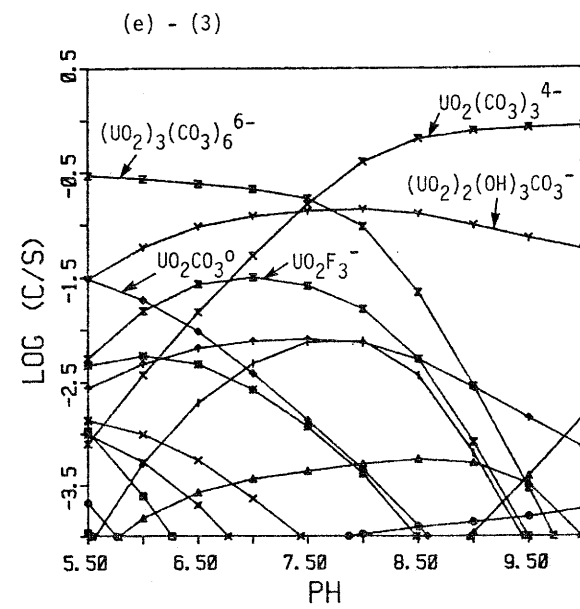
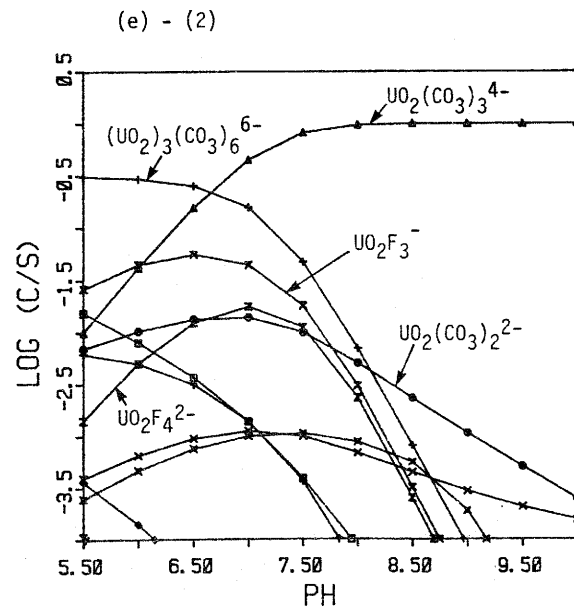
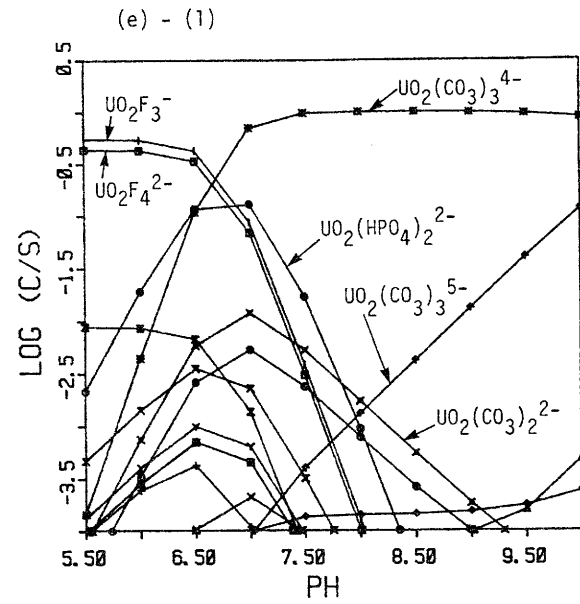
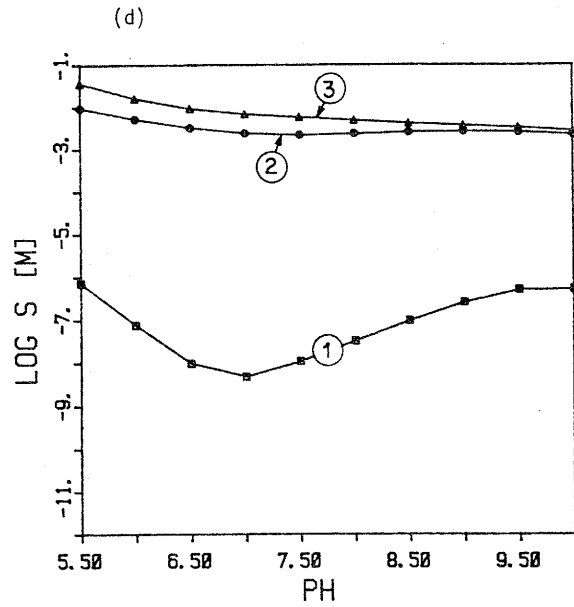
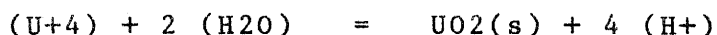


Figure 9 (continued)

The variation of the thermodynamic database (compare Figs. 6 and 8) leads to considerable changes for predicted solubility in reducing environment and for uranium speciation in general. As summarized in Fig. 10, Allard's database (B) yields concentration limits which are at least three orders of magnitude higher than the corresponding values for the boundaries of the reducing environment obtained with database A. The primary reason is the difference in stability attributed to UO₂(s). The log K value for reaction



is set to 0.6 in database A and to 4.6 in database B (Fig. 3). Because UO₂(s) is the limiting solid for both Eh/pH conditions and for both databases (subfigures (a)), the maximum uranium aquo ion activities are four orders of magnitude higher with database B, implying a comparable solubility difference at fixed Eh and pH.

A comparison of the speciation pattern (subfigures (e-1) to (e-3)) clearly depicts that Allard's database emphasizes the formation of U(VI) carbonate and fluoride complexes (Appendix A, Table A-7).

Allard (1983) did not correct for ionic strength effects stating that the error introduced is small compared to the uncertainty of the thermodynamic data themselves. Large ionic strength effects are possible whenever the mass action law of the solubility-limiting reaction has, at specified pH and Eh, a large activity coefficient correction term; such conditions are usually associated with the appearance of highly charged species and/or large stoichiometric coefficients.

As a check, comparative calculations were performed with Allard's database (B), setting ionic strength either equal to 0.2 (Fig. 8) or equal to 0 (Fig 9), the latter condition reflecting Allard's concept. The effect of ionic strength is small for the upper Eh limit of the depth environment (lines (2)), but changing ionic strength from 0 to 0.2 causes a solubility increase of more than one order of magnitude at the lower Eh boundary (lines (1)) for pH >6, as depicted by Fig. 10. These variations are in fact less than the differences which would result if we consider extremes of reported UO₂ solubility constants in Fig. 3 (difference of 10 orders of magnitude).

3.2.2 Validation

Figure 10 depicts uranium concentrations reported for natural groundwaters, either explicitly plotted as a function of pH or simply given as range in cases where no pH data are available. The concentration range for uranium in reducing groundwaters

given by Osmond and Cowart (1976) agrees well with the values observed in Swiss groundwaters and in deep granitic waters from Sweden, which are, typically, of the order of 0.1 to 10 ppb.

These experimental points are well bracketed by the solubility lines computed for the assumed upper and lower Eh boundary of the depth environment with database A for 25 C and ionic strength 0.2, suggesting that

(1) most of the analysed waters could, as expected, represent uranium-saturated solutions under reducing conditions at 25 C;

(2) line (A2) might be a reasonable estimate for upper uranium concentration limits for deep groundwaters at low temperatures, as even the extreme Finnish waters fit fairly well in this model provided their pH is above 8.

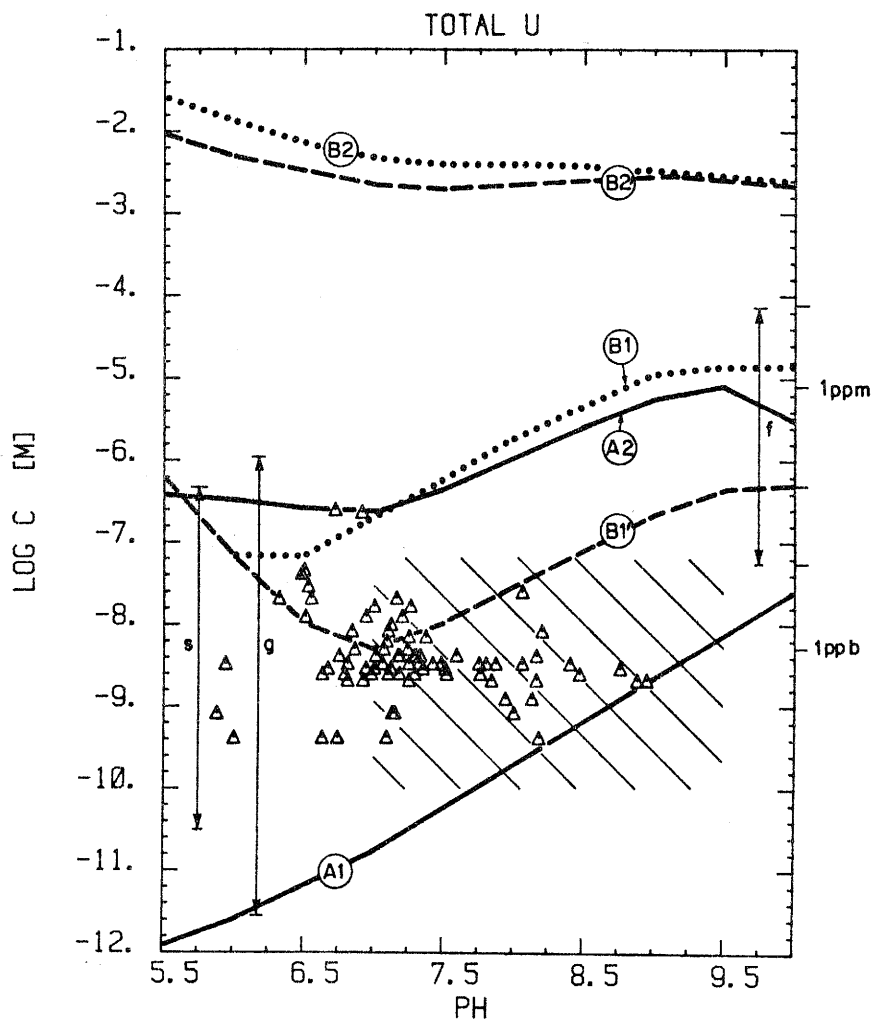
Reported uranium contents lie, on the other hand, at or below maximum solubilities computed with Allard's database (B) for the assumed low Eh boundary (lines (B1) or (B1')). Most of the solutions would, therefore, be undersaturated with respect to uranium. For the upper Eh boundary, the solubilities are extremely high (lines (B2) and (B2')) and so far without experimental support. Hence, line (A2) is tentatively selected as representative for upper uranium concentration limits in granitic waters under reducing conditions.

Figure 10 : Summary of computed uranium solubilities at 25 C and comparison to observations.

Theoretical lines are representative for cases :

- A1 - database A, I=0.2, Eh[mV]= 220 - 59 pH
- A2 - database A, I=0.2, Eh[mV]= 407 - 59 pH
- B1 - database B, I=0.2, Eh[mV]= 220 - 59 pH
- B2 - database B, I=0.2, Eh[mV]= 407 - 59 pH
- B1' - database B, I=0.0, Eh[mV]= 220 - 59 pH
- B2' - database B, I=0.0, Eh[mV]= 407 - 59 pH

Observations are given as : triangles for data from wells in northern Switzerland (NAGRA (1981)); hatched area for Swedish granitic groundwaters (Allard (1983)); concentration ranges for surface waters (s) and groundwaters (g) from Osmond and Cowart (1976) and for anomalously uranium-rich finnish groundwaters (f) reported by Asikainen (1979).



3.3 Neptunium

3.3.1 Presentation

Neptunium solubility and speciation in the reference water was computed for both databases at 25 C and ionic strength 0.2 (Figs. 11 and 12). Calculations for 75 C were omitted since no enthalpy data for dissolved Np species are available in any of the databases.

Figures 11 and 12. Neptunium solubility and speciation in reference water.

Following cases are considered :

<u>figure</u>	<u>database</u>	<u>temperature</u>	<u>ionic strength</u>
11	A	25 C	0.2
12	B	25 C	0.2

Following plots are shown in one figure :

(i) as a function of pH and Eh :

- (a) solubility limiting phase
- (b) dominant dissolved species
- (c) solubility isopleths (log. units; star denotes minimum, triangle maximum value)

(ii) as a function of pH :

- (d) solubility S
- (e) speciation (species concentration / solubility; only species above 1 % level specified)

for three selected Eh/pH relationships :

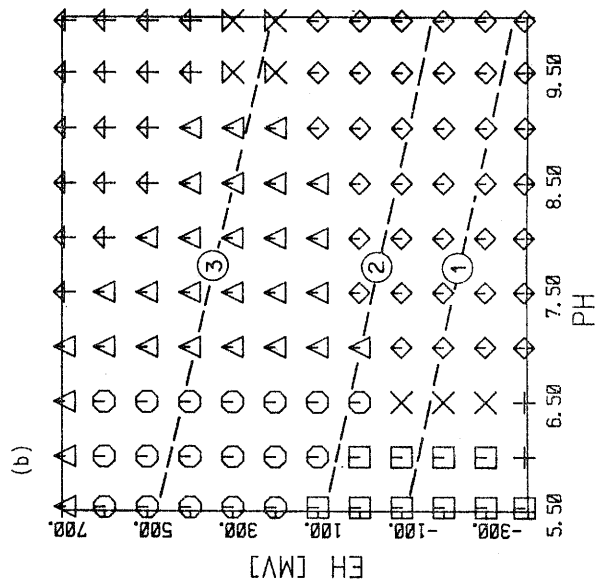
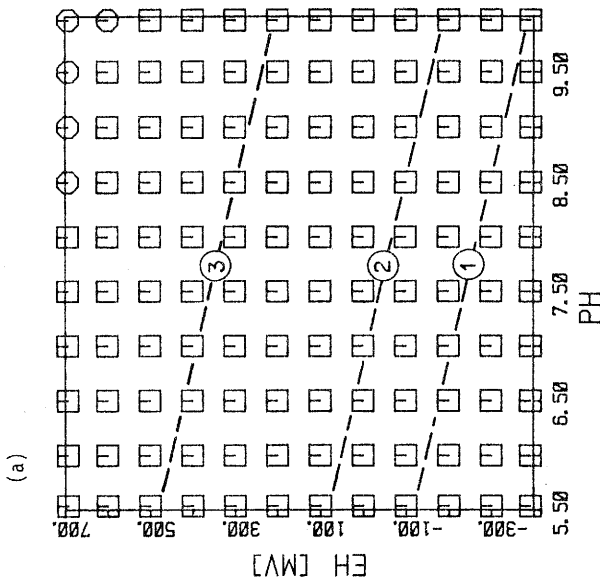
- (1) Eh[mV] = 220 - 59 pH
- (2) Eh[mV] = 407 - 59 pH
- (3) Eh[mV] = 800 - 59 pH

Figure 11

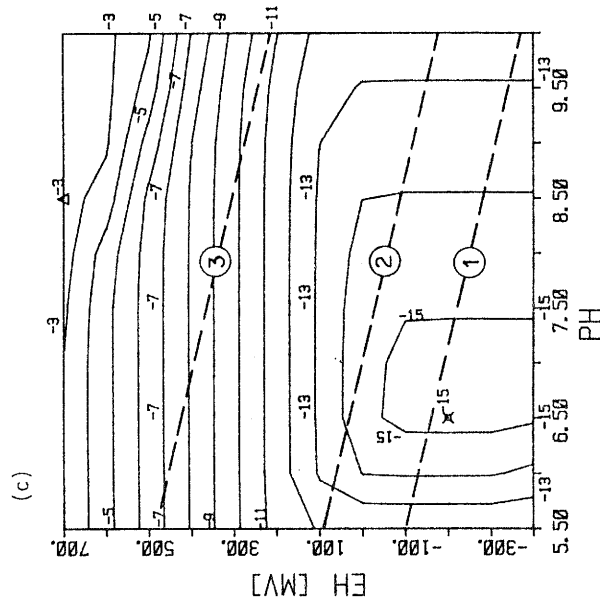
db = A, T = 25 C, I = 0.2

Np

- \square $\text{NpO}_2(\text{s})$
- \circ $\text{NpO}_2(\text{OH})_2(\text{s})$



- \square NpF_4^0
- \circ $\text{NpO}_2(\text{HCO}_3)_0$
- \triangle NpO_2^+
- $+$ NpCO_3^+
- \times $\text{Np}(\text{OH})_4^0$
- \diamond $\text{Np}(\text{OH})_5^-$
- \leftarrow $\text{NpO}_2(\text{CO}_3)_3^{4-}$
- \times NpO_2OH^0



Eh/pH functions :

- (1) Eh(mv) = 220 - 59 pH
- (2) Eh(mv) = 407 - 59 pH
- (3) Eh(mv) = 800 - 59 pH

Np

db = A, T = 25 C, I = 0.2

Eh/pH functions :

- (1) Eh(mV) = 220 - 59 pH
- (2) Eh(mV) = 407 - 59 pH
- (3) Eh(mV) = 800 - 59 pH

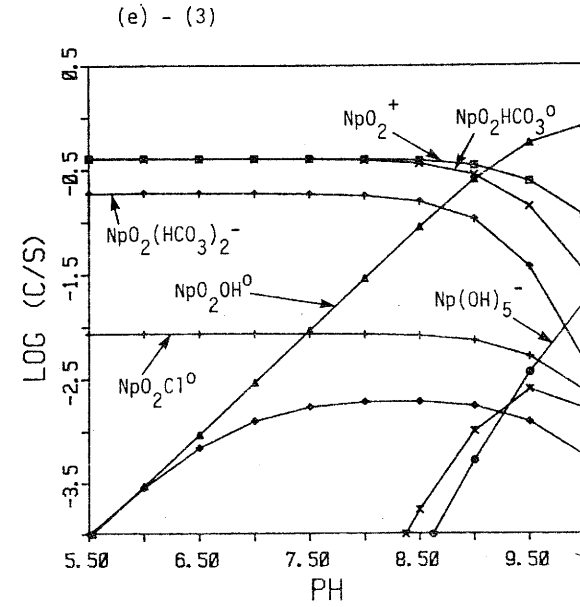
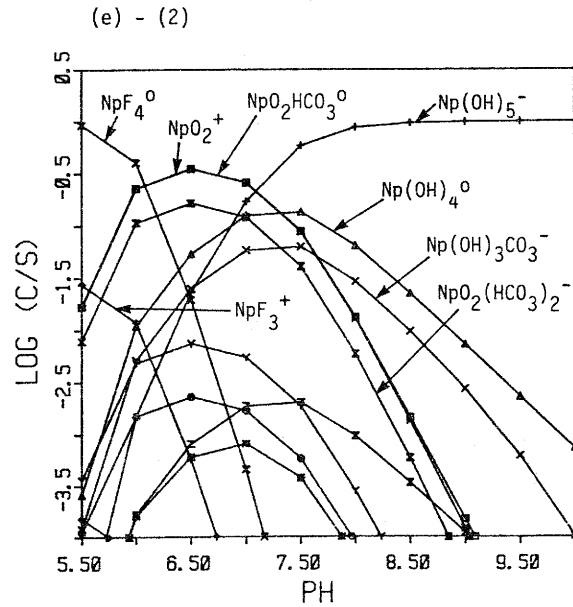
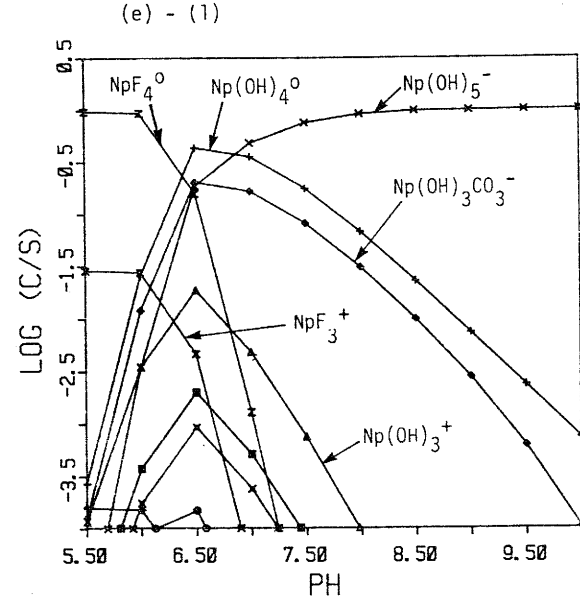
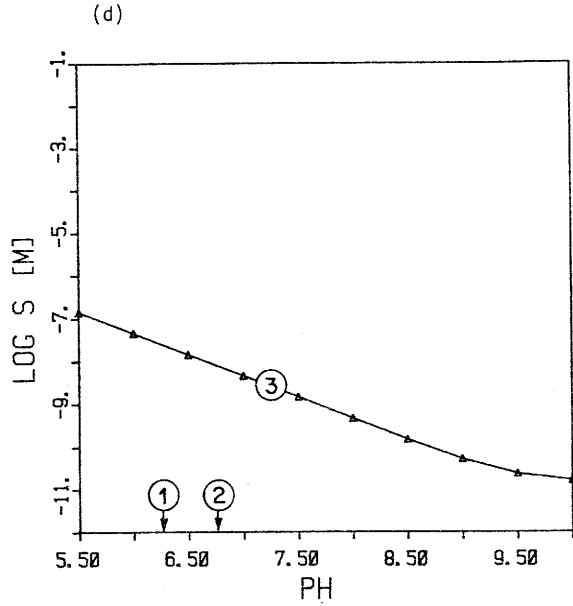
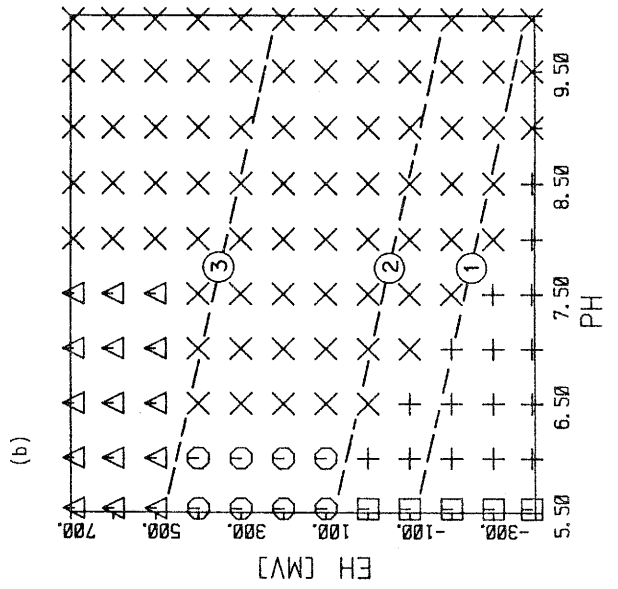
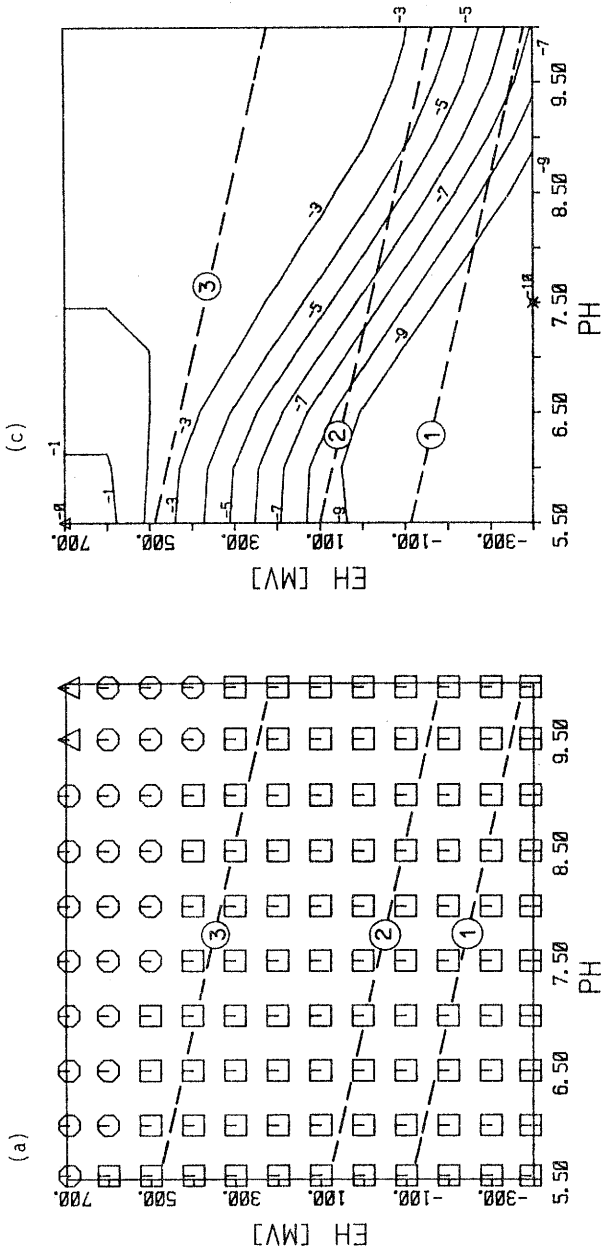


Figure 12

db = B, T = 25 C, I = 0.2

Np

- $\text{NpO}_2(\text{s})$
- $\text{NpO}_2\text{OH}(\text{s})$
- △ $\text{NpO}_2(\text{OH})_2(\text{s})$



- $\text{Np}(\text{HPO}_4)_3^{2-}$
- $\text{NpO}_2\text{F}^{\ominus}$
- △ NpO_2^+
- +
- × $\text{Np}(\text{OH})_4^{\ominus}$
- × $\text{NpO}_2(\text{CO}_3)_3^{5-}$

Eh/pH functions :

- (1) Eh (mV) = 220 - 59 pH
- (2) Eh (mV) = 407 - 59 pH
- (3) Eh (mV) = 800 - 59 pH

Np

db = B, T = 25 C, I = 0.2

Eh/pH functions :

- (1) Eh(mV) = 220 - 59 pH
- (2) Eh(mV) = 407 - 59 pH
- (3) Eh(mV) = 800 - 59 pH

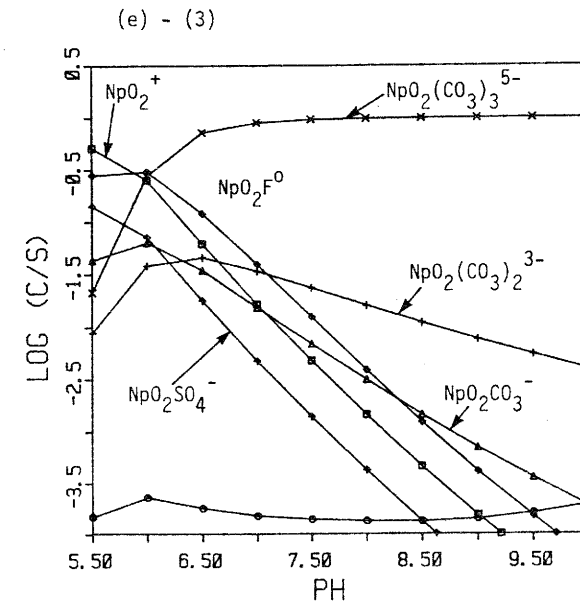
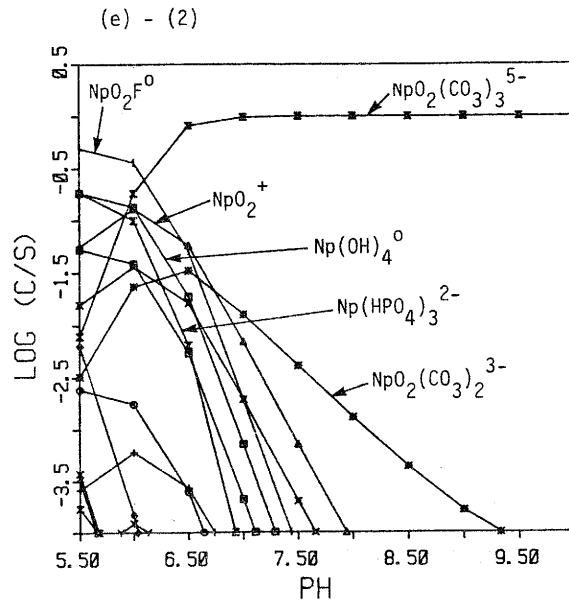
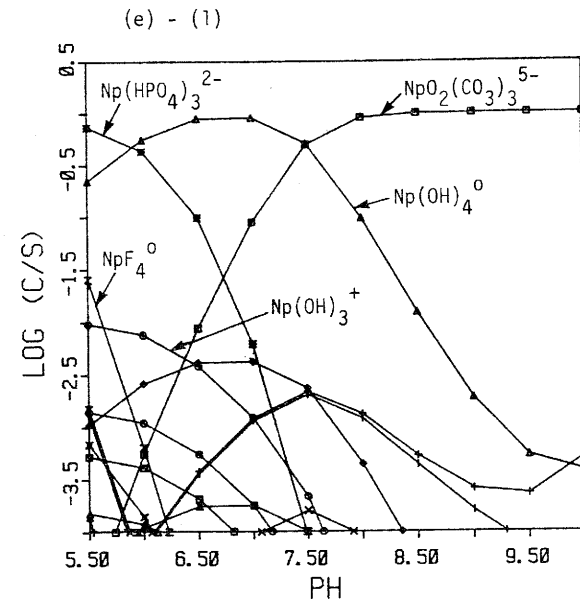
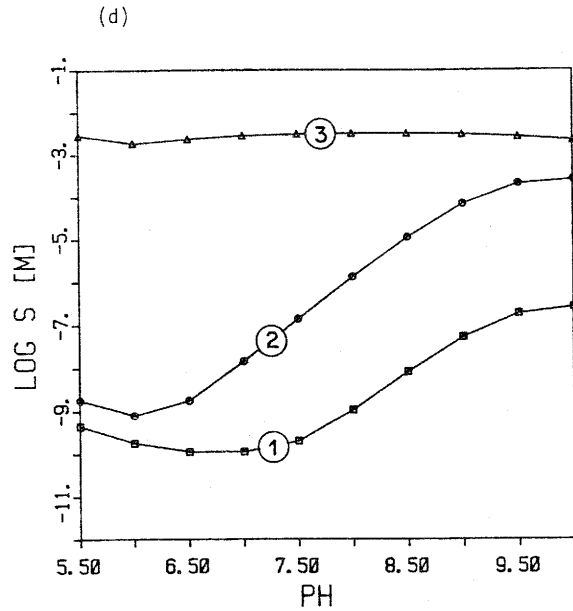
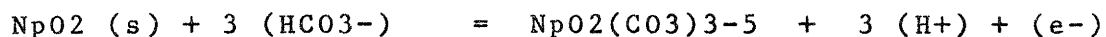


Figure 12 (continued)

It should be emphasized that the reliability of the formation constants for Np species is considered as particularly poor. Appendix A reveals important differences for the log K values of many species when comparing databases A and B (e.g. for $\text{Np}(\text{OH})_3^+$, $\text{Np}(\text{OH})_4$, $\text{NpO}_2(\text{s})$, $\text{Np}(\text{IV})$ -sulphate complexes); in addition, database A does not include $\text{Np}(\text{IV})$ -phosphate complexes and the $\text{Np}(\text{V})$ -carbonate species are defined differently.

This implies large differences between the isosolubility plots (subfigures (c)), although both datasets dominantly take $\text{NpO}_2(\text{s})$ as limiting solid (subfigures (a)). Database A, which has been used previously at EIR (Schweingruber (1981,1982a)), predicts extremely low Np solubilities in reducing environments (as low as $1\text{E}-15$ M). The solubility minimum observed with base B is in the order of $1\text{E}-10$ M, and the solubility may be up to 10 orders of magnitude higher than with base A (e.g. lines (3) at high pH in subfigures (d)).

It's important to note that the formation of extremely high charged species such as $\text{NpO}_2(\text{CO}_3)_3^{5-}$ (dominant in a large part of the Eh/pH field, see Fig. 12(b)) is very sensitive to ionic strength corrections. The formation of that species may be expressed by redox reaction



with the corresponding Nernst equation at 25 C

$$\log\{\text{NpO}_2(\text{CO}_3)_3^{5-}\} = (\text{E}_0 - \text{E}_h)/59 + 3 \text{ pH} + 3 \log\{\text{HCO}_3^-\} .$$

With the logarithm of the activity coefficient of a single-charged ion at ionic strength 0.2 from Table B-1 in Appendix B (-.1345) and assuming the equivalence of total carbonate and bicarbonate concentration we derive

$$\log[\text{NpO}_2(\text{CO}_3)_3^{5-}] = (\text{E}_0 - \text{E}_h)/59 + 3 \text{ pH} + 3 \log[\Sigma \text{CO}_3] + (3 \cdot -25) \cdot (-.1345) .$$

Hence, the concentration of that Np species at fixed Eh, pH and total carbonate concentration is calculated to be about 3 orders of magnitude higher than without ionic strength correction (i.e. omitting the last term of the last eq.). This is a major reason (another being the higher total carbonate content of the reference water) why solubility curve (2) in Fig. 12 lies far above the solubility Allard (1983) indicated for a similar Eh/pH relationship (his figure 6b).

The question may be posed whether such high-charged species are realistic in aqueous solutions, since one would expect them to be more or less tightly associated with counter-ions lowering the net charge of the complex. This effect would, of course, invalidate the simple modelling approach for activity coeffi-

lients. It is used here, however, as this treatment clearly leads to solubility overestimation.

3.3.2 Validation

Literature data on dissolved Np under strongly reducing conditions have not been found so far. However, an evaluation of Np solubilities under rather oxidizing conditions seems to be possible from a series of laboratory experiments.

Rai et al. (1982) investigated Np concentrations in CaCl₂ solutions contacting Np-doped glass (with or without addition of crystalline NpO₂), with pH varying from 4.5 to 6.5. Quinhydrone was added to buffer the redox potential Eh at (696 -59 pH) mV, i.e. on a parallel about 100 mV below line (3) in Figs. 11(c) and 12(c). For the pH range 5.5 to 6.5, they reported Np concentrations around 2E-6 M in filtered samples. These observations contradict the predictions of database A but are consistent with those of database B.

Rai et al. (1982) cite results from static Np leach tests performed at PNL with the same glass, once with distilled water (final pH about 8) and once with a 0.015 M NaHCO₃ solution (pH around 9), the system being open to the atmosphere. The reported steady-state concentrations are displayed in Fig. 13. Olofsson et al. (1983b) demonstrated that Np concentrations of 2.1E-7 M are quite stable in aerated 0.01 M NaClO₄ solutions over a pH range 5.5 to 10. These observations suggest that line (A3) is not a conservative estimate for maximum Np solubility under oxic conditions.

Susak et al. (1983) reported that the interaction of Np(VI) in 0.1 M NaHCO₃ solution, distilled water, or artificial seawater with or without contacting basalt or olivine results in the production of Np(V) and Np(IV). Reaction kinetics were investigated over a period of 120 to 140 days, starting with initial Np concentrations of 1E-3 to 2E-3 M. Their data on final pH and speciation suggest that Np is dominantly kept in solution in the case of the bicarbonate solvent (pH 8.9) as a mixture of Np(V) and Np(VI). A Np loss of up to 50 % due to solid formation was observed for distilled water (final pH 7.6). It is difficult to validate our model with these observations, since no indication is given for Eh and chemical equilibrium is not guaranteed. Assuming near-equilibrium conditions slightly below Eh/pH relationship (3), we would nevertheless get a fair consistency with the predictions obtained for database B (Fig. 12). Their results do, however, not conform to Fig. 11(c).

Cleveland et al. (1983a) stated that about 15 to 95 % of either Np(V) or Np(IV) contained in 1E-8 molar groundwater solutions remained dissolved after 17 to 30 days. Np(V) was the only oxidation state detected in solution, and insoluble Np was reported to be Np(IV). Their observations are in better agreement with the predictions based on dataset A, provided the actual redox potential was similar to the one proposed as Eh/pH

function (3). They could be consistent with Fig. 12(c) if reducing conditions had been established.

Apparently, it's impossible to discriminate between the reliability of databases A and B from the above discussion. For conservative reasons, database B is provisionally selected to derive recommendations on maximum Np solubilities. Figure 13 depicts that the limits for reducing and oxidic conditions advocated in the most recent Swedish safety report (KBS-3 (1983)) are slightly below curves (B2) and (B3).

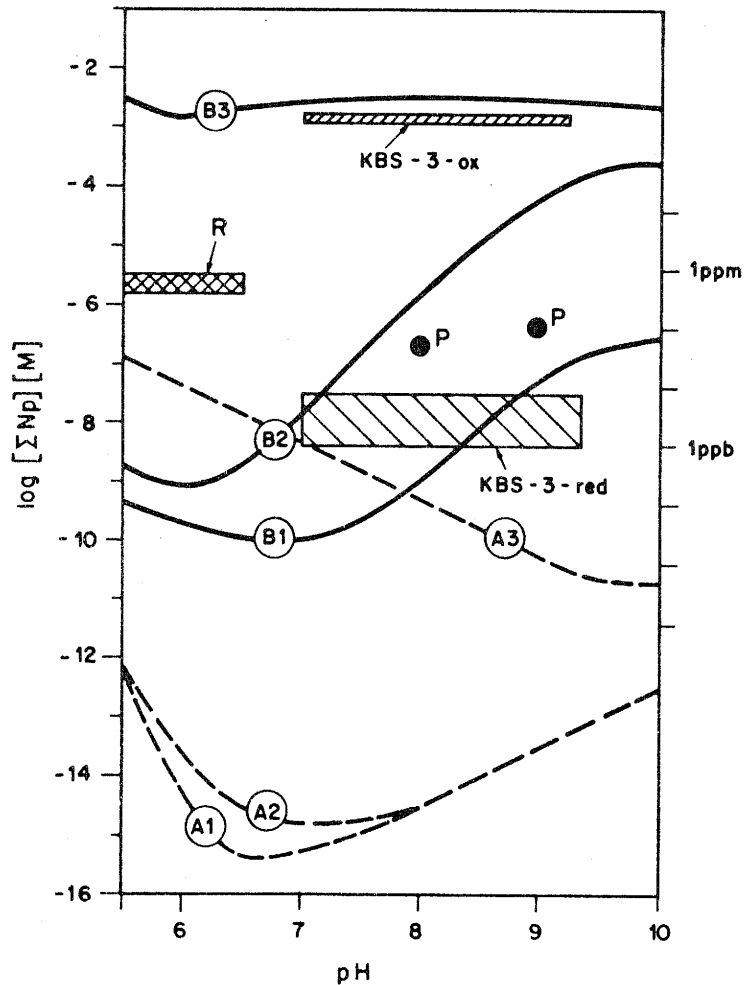
Figure 13 : Summary of computed neptunium solubilities at 25 C and comparison to observations.

Theoretical lines are representative for cases :

- A1 - database A, I=0.2, Eh[mV]= 220 - 59 pH
- A2 - database A, I=0.2, Eh[mV]= 407 - 59 pH
- A3 - database A, I=0.2, Eh[mV]= 800 - 59 pH
- B1 - database B, I=0.2, Eh[mV]= 220 - 59 pH
- B2 - database B, I=0.2, Eh[mV]= 407 - 59 pH
- B3 - database B, I=0.2, Eh[mV]= 800 - 59 pH

Observations are given as : R - glass-leaching experiments of Rai et al. (1982); P - PNL data cited by Rai et al. (1982).

Limits used in Swedish safety report KBS-3 (1983) for reducing (red) and oxidizing (ox) conditions.



3.4 Plutonium

3.4.1 Presentation

The results of three case studies are collected in Figs. 14 to 16. From the corresponding subfigures one notes :

(a) $\text{PuO}_2(\text{s})$ is predicted to be the limiting solid for the Eh/pH range and temperature interval considered, except for the high Eh/pH corner in Figs. 15(a) and 16(a), where $\text{PuO}_2(\text{OH})_2$ is less soluble.

Figures 14 to 16. Plutonium solubility and speciation in reference water.

Following cases are considered :

<u>figure</u>	<u>database</u>	<u>temperature</u>	<u>ionic strength</u>
14	A	25 C	0.2
15	A	75 C	0.2
16	B	25 C	0.2

Following plots are shown in one figure :

(i) as a function of pH and Eh :

(a) solubility limiting phase
(b) dominant dissolved species
(c) solubility isopleths (log. units; star denotes minimum, triangle maximum value)

(ii) as a function of pH :

(d) solubility S
(e) speciation (species concentration / solubility;
only species above 1 % level specified)

for three selected Eh/pH relationships :

- (1) Eh[mV] = 220 - 59 pH
- (2) Eh[mV] = 407 - 59 pH
- (3) Eh[mV] = 800 - 59 pH

Pu

db = A, T = 25 C, I = 0.2

Eh/pH functions :

- (1) Eh(mV) = 220 - 59 pH
- (2) Eh(mV) = 407 - 59 pH
- (3) Eh(mV) = 800 - 59 pH

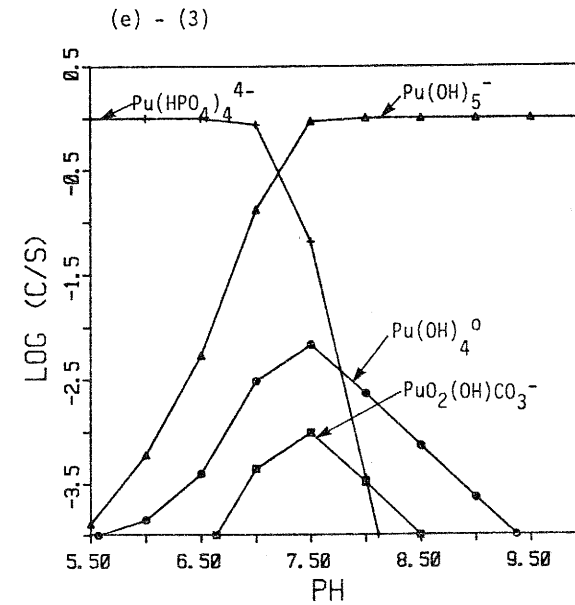
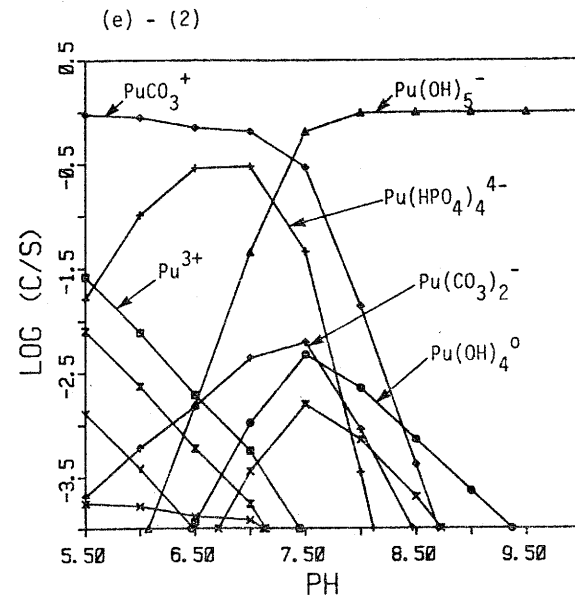
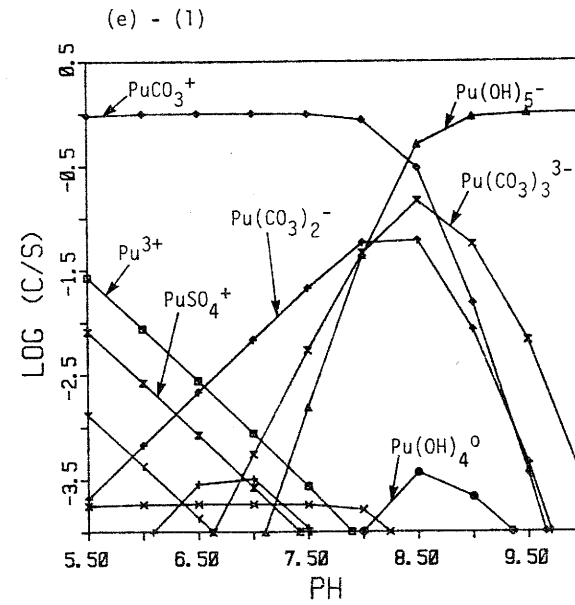
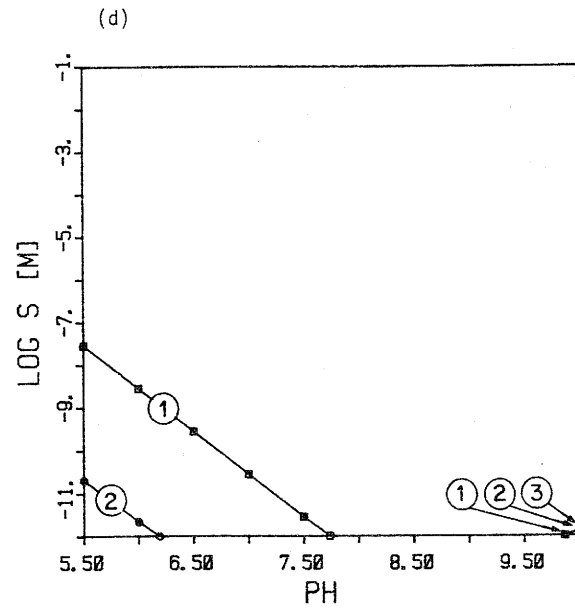
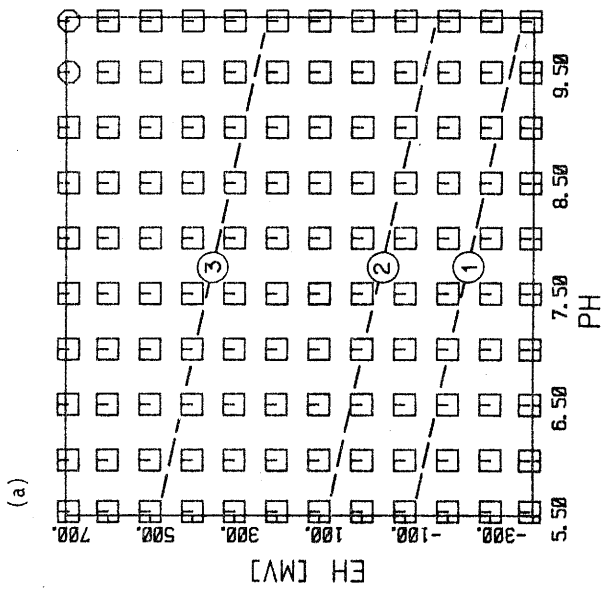
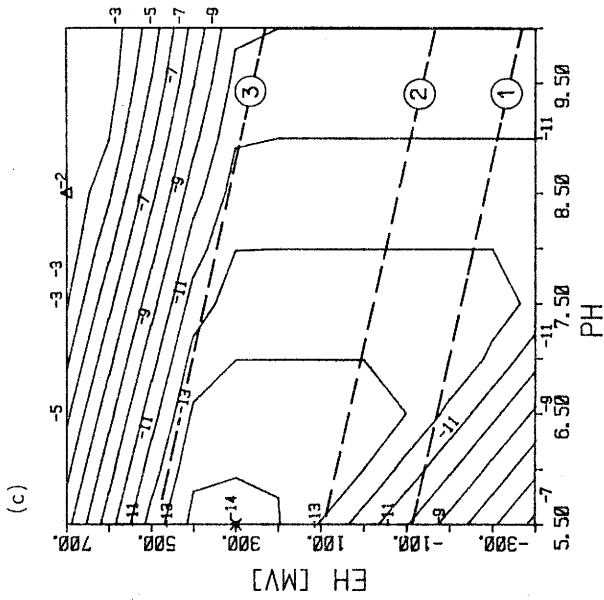


Figure 14 (continued)

Figure 15

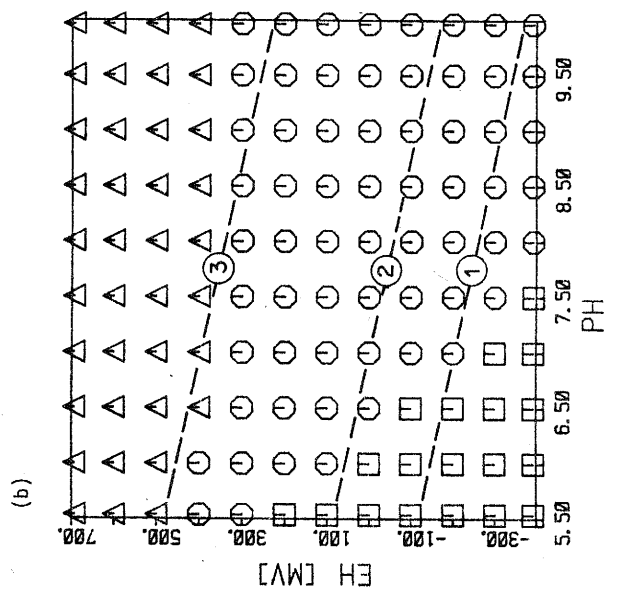
db = A, T = 75 C, I = 0.2

Pu



- \square $\text{PuO}_2(s)$
- \circ $\text{PuO}_2(\text{OH})_2(s)$

- Eh/pH functions :
- (1) $\text{Eh}(\text{mV}) = 220 - 59 \text{ pH}$
 - (2) $\text{Eh}(\text{mV}) = 407 - 59 \text{ pH}$
 - (3) $\text{Eh}(\text{mV}) = 800 - 59 \text{ pH}$



- \square PuCO_3^+
- \circ $\text{Pu}(\text{OH})_5^-$
- \triangle $\text{PuO}_2(\text{OH})\text{CO}_3^-$

Pu

db := A, T = 75 C, I = 0.2

Eh/pH functions :

- (1) Eh(mV) = 220 - 59 pH
- (2) Eh(mV) = 407 - 59 pH
- (3) Eh(mV) = 800 - 59 pH

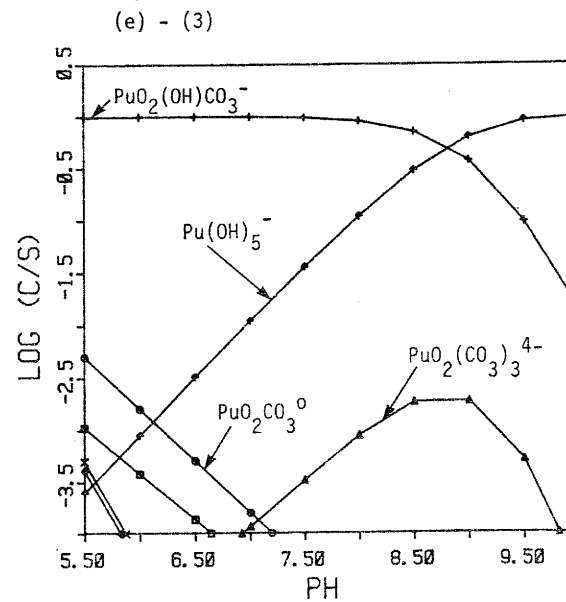
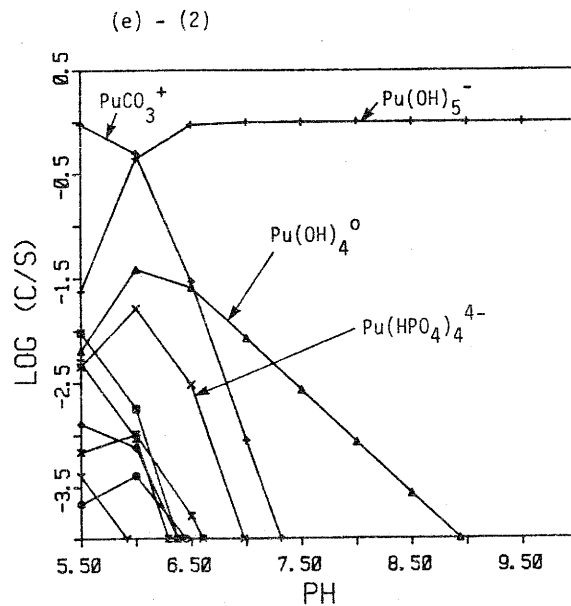
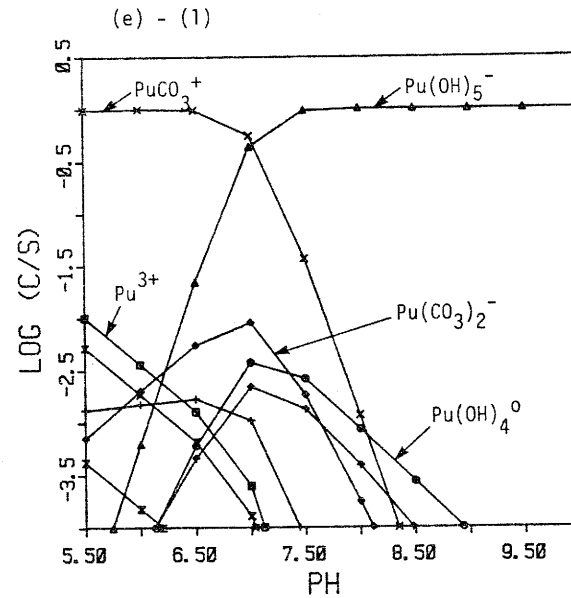
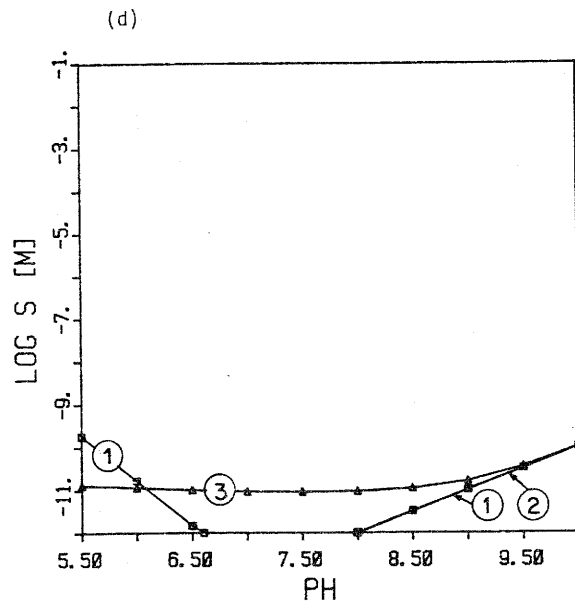
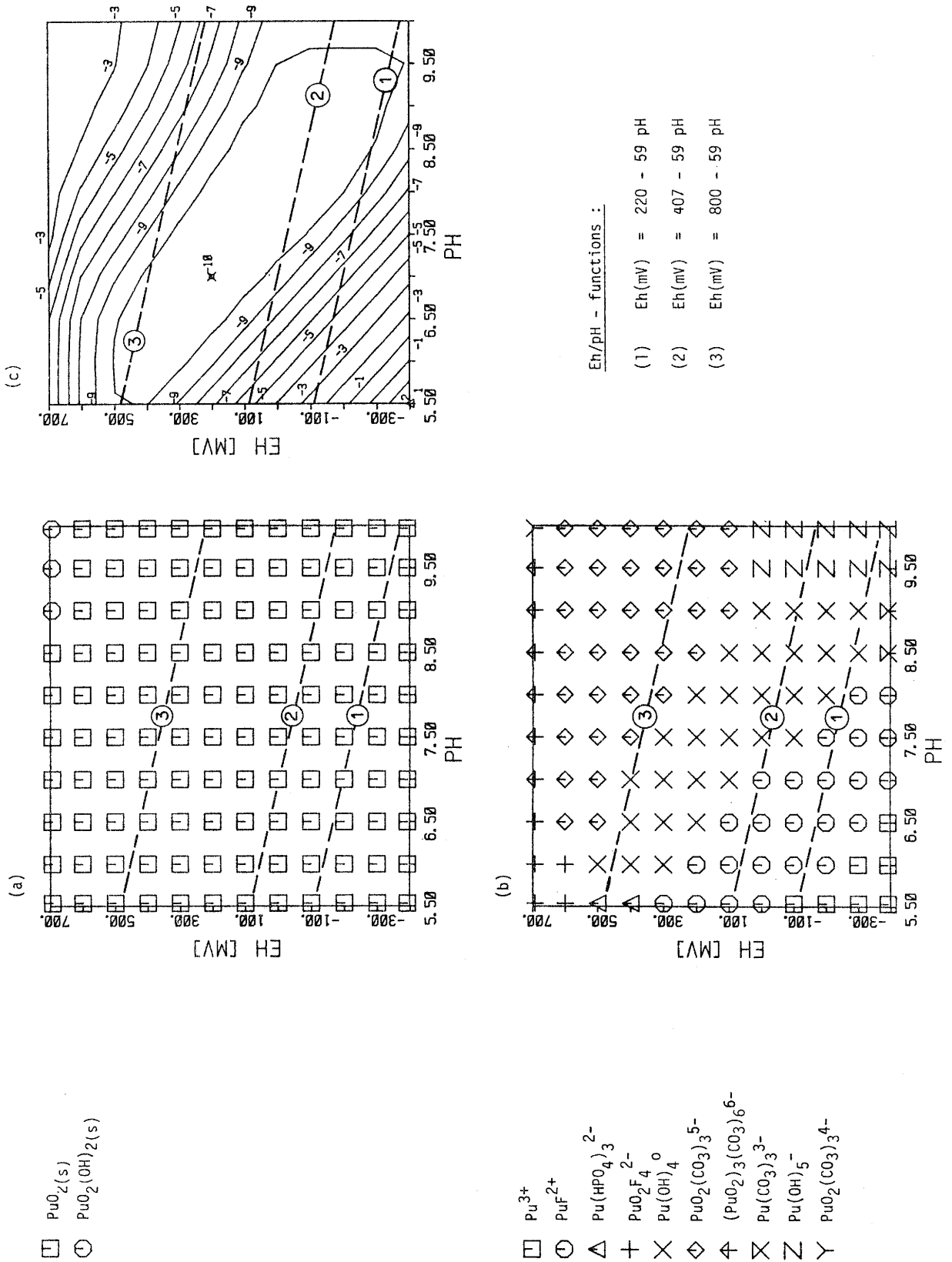


Figure 15 (continued)

Figure 16

db = B, T = 25 C, I = 0.2

Pu



Pu

db = B, T = 25 C, I = 0.2

Eh/pH functions :

(1) Eh(mV) = 220 - 59 pH

(2) Eh(mV) = 407 - 59 pH

(3) Eh(mV) = 800 - 59 pH

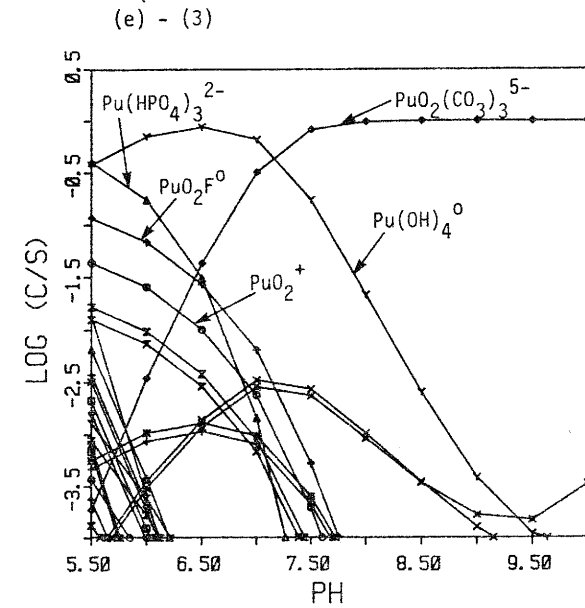
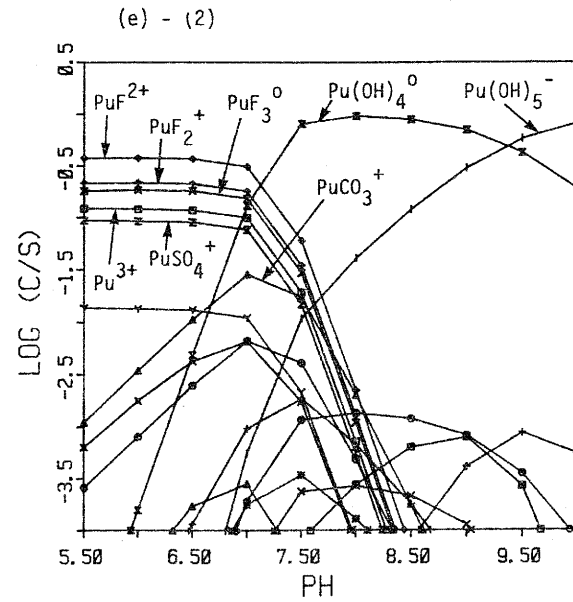
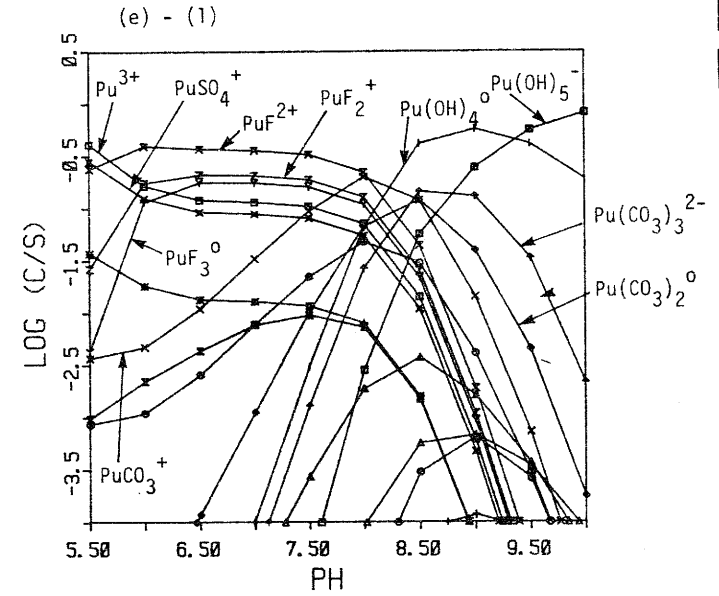
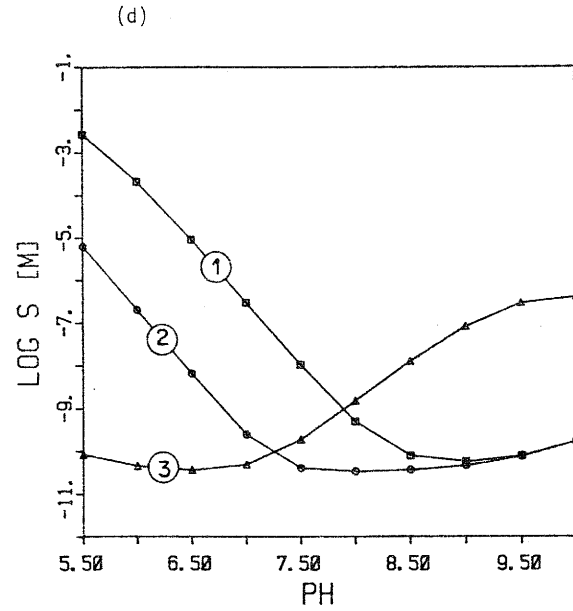


Figure 16 (continued)

(b) Oxidation states III (lower pH values) and IV are calculated to dominate under reducing, and IV, V and VI under oxic conditions.

(c) The isosolubility curves depict a solubility minimum in the area of Pu(IV) predominance in solution. Eh/pH functions (2) and (3) bracket a zone of low solubility, whereas solubility is increased under very reducing conditions (function (1)). The differences between the predictions of bases A and B at 25 C (Figs. 14(c) and 16(c)) arise from the large difference attributed to the stability of PuO₂(s). The corresponding K value in database A is six orders of magnitude above that of base B (Fig. 3), yielding comparable solubility decreases.

(d) The solubilities computed for the three Eh/pH relationships are extremely low with data from base A, being lower than 1E-12 M for a large pH range. A temperature shift from 25 to 75 C tends to decrease solubility under reducing conditions at low pH values and yields a solubility increase for all other conditions (see also Fig. 17).

(e) Speciation diagrams 14(e) and 16(e) reveal important differences between the two datasets. Base A does take the formation of Pu(III) fluoride and Pu(V) carbonate complexes into account, and the stability of Pu(OH)₅⁻ is assumed to be much higher (cf. Appendix A).

3.4.2 Validation

Figure 17 contains a summary of Pu solubility curves for Eh/pH functions (1) and (3). The former should be representative of upper concentration limits under reducing groundwater conditions (see Figs. 14(c) and 16(c)), while the latter will be used for a first model validation.

Rai et al. (1977) conducted solubility experiments with PuO₂(s) in 0.003 N CaCl₂ solutions under atmospheric conditions with varying pH. The two points indicated in Fig. 17 represent dissolved Pu concentrations observed after 90 a days' contact with PuO₂(s), the samples being centrifuged and filtered through a 0.015 um filter. DeRegge et al. (1979) describe Pu adsorption experiments on clay under oxic conditions; the solubility of PuO₂(s) was investigated in preliminary experiments. Fig. 17 also includes concentrations of dissolved Pu remaining from an initial content of 6E-8 M in a 0.01 M NaClO₄ solution at various pH values (Olofsson et al. (1983b)). Cleveland et al. (1983b) studied the fate of 1E-9 M Pu dissolved in four groundwaters at two temperatures (25 and 75 C), with a maximum observation period of 30 days.

The interpretation of these experimental results is, however, difficult due to

- lack of information on experimental Eh;

- the tendency of Pu(IV) to form metastable colloids or pseudocolloids (adsorption on colloidal material already present in solution) in near-neutral aqueous solutions (discussed e.g. by Andelman and Rozzell (1970), Nishita (1979)).

Assuming that (i) Eh/pH function (3) is representative of the laboratory conditions and that (ii) the reported concentrations indeed refer to non-colloidal dissolved species, both datasets fail to predict conservative estimates for Pu solubility limits under oxic conditions. Note however that most points would fall below the solubility curve for base B if the redox potential is in fact 200 mV higher (Fig. 16(c)); this would not be true for dataset A (Fig. 14(c)).

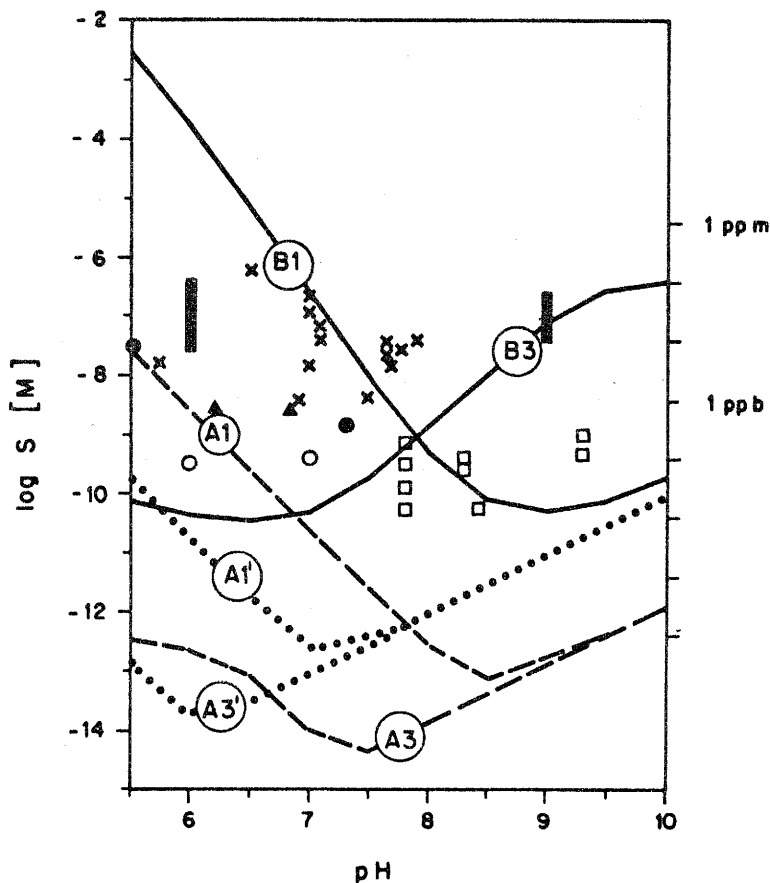
The ultimate choice of curve (B1) as conservative solubility limit for reducing groundwater environments is speculative, and its reliability is uncertain. Note that the limits adopted in KBS-3 (1983) for pH interval 7 to 9 are approximately equal to the maximum values for curves (B1) and (B3) in Fig. 17, respectively: the Swedes use constants of 3 mg/l (or $1E-4.9$ M) and of 8 ug/l (or $1E-7.5$ M) to define Pu solubility limits under reducing and oxidizing conditions. The latter limit would, in fact, be consistent with the experimental data points of Fig. 17.

Figure 17: Summary of computed plutonium solubilities for $I=0.2$ and comparison to observed concentrations.

Theoretical lines are representative for cases :

- A1 - database A, T= 25 C, Eh [mV] = 220 - 59 pH
- A3 - database A, T= 25 C, Eh [mV] = 800 - 59 pH
- A1' - database A, T= 75 C, Eh [mV] = 220 - 59 pH
- A3' - database A, T= 75 C, Eh [mV] = 800 - 59 pH
- B1 - database B, T= 25 C, Eh [mV] = 220 - 59 pH
- B3 - database B, T= 25 C, Eh [mV] = 800 - 59 pH

Concentrations reported for centrifuged and/or filtered solutions : 0.003 N CaCl₂ solutions after 90 days' contact with PuO₂(s) (full circles, Rai et al. (1977)); PuO₂(s) dissolution in Belgian groundwater at fixed pH (bars) and in a water containing soluble clay components (triangles; both DeRegge et al. (1979)); final concentrations in adsorption experiments on clay after thermal and irradiation treatment (crosses; DeRegge et al. (1979)); 0.01 M NaClO₄ with initial Pu concentration 6E-8 M (open circles, Olofsson et al. (1983b)); various groundwaters with 1E-9 M total Pu concentrations after 30 days reaction time (squares; Cleveland et al. (1983b)).



3.5 Americium

3.5.1 Presentation

Americium solubility and speciation in the reference water was modelled for 25 C only (Fig. 18) since no enthalpy data were available. Note from Table A-4 in Appendix A that most equilibrium constants for Am species are speculative (estimates, extrapolated values). Since Am(III) is the only oxidation state considered, the results are identical for all Eh/pH functions listed in Table 1.

Case studies (I) and (II) rely on the assumed nature of limiting solids used so far (i.e. only Am(OH)₃ (s) considered) and basically serve to compare databases A and B. Since equilibrium solutions turned out to be strongly oversaturated with respect to the carbonate solid (Am₂(CO₃)₃ (s)), this phase was tentatively included in case study (III). Here, the carbonate system was not considered to be strictly closed. The change in total carbonate due to solid carbonate dissolution was, however, minimal. Note that this calculation is not conservative since Am solubility is depressed by the extremely high total carbonate content assumed.

If solubility is exclusively determined by the hydroxide, both databases predict very high Am concentrations below pH 7.5 such that saturated solutions cannot be obtained within the preset ionic strength limit. The corresponding solubility and speciation plots are, therefore, cut off for pH < 7.5. The most significant difference between the datasets is that database (B) takes carbonate complexes into account, which become important for pH > 7.5 and raise solubility.

A considerable solubility reduction is obtained if the carbonate solid is included as potential limiting solid. This phase is indeed more stable than the hydroxide below a pH of about 10 (Fig. 18(a)). Fig. 18(b)-(III) shows that fluoride and sulphate complexes should be of great importance in neutral or slightly acidic waters.

Generally, a fairly large number of complexes are predicted to coexist in comparable amounts (only the most important ones are specified in Fig. 18). Cationic and neutral species are dominant over the entire pH interval with database A; anionic species are important for pH > 8.5 with database B.

3.5.2 Validation

Laboratory experiments investigating the formation of actinide colloids in sodium perchlorate media open to the atmosphere (Olofsson et al. (1983b)) suggest that Am concentrations in the order of 10^{-7} to 10^{-8} M are stable within pH range 5.5 to 10. Cleveland et al. (1983a) investigated Am behaviour when added to various groundwaters (pH range 7.8 to 9.3) at $1E-11$ and $1E-8$ molar levels. They conclude (i) that their apparent solubilities are not saturation-limited and (ii) that dissolved Am is indeed affected by the fluoride content.

These observations do not contradict any of the solubility curves of Fig. 18(a) and are therefore not suitable to discriminate between model curves (I) to (III).

The maximum Am concentration taken as reference in KBS-3 (1983) was 6 ppm for pH interval 7 to 9. This value corresponds to the maximum value of curve (III) within that pH range, and represents an intermediate number with respect to curves (I) and (II). For purely conservative reasons, line (II) is provisionally proposed to describe upper Am concentration limits.

Figure 18: Americium solubility and speciation in reference water. Curves are valid for Eh range -400 to 700 mV.

Following cases are considered :

case	database	temperature	ionic strength	solids
----	-----	-----	-----	-----
I	A	25 C	0.2	Am(OH) ₃
II	B	25 C	0.2	Am(OH) ₃
III	B	25 C	0.2	Am(OH) ₃ Am ₂ (CO ₃) ₃

Plots given as a function of pH :

- (a) solubility S
- (b) speciation (species concentration / solubility)
with indication of limiting solid

Am

Eh interval : -400 to 700 mV

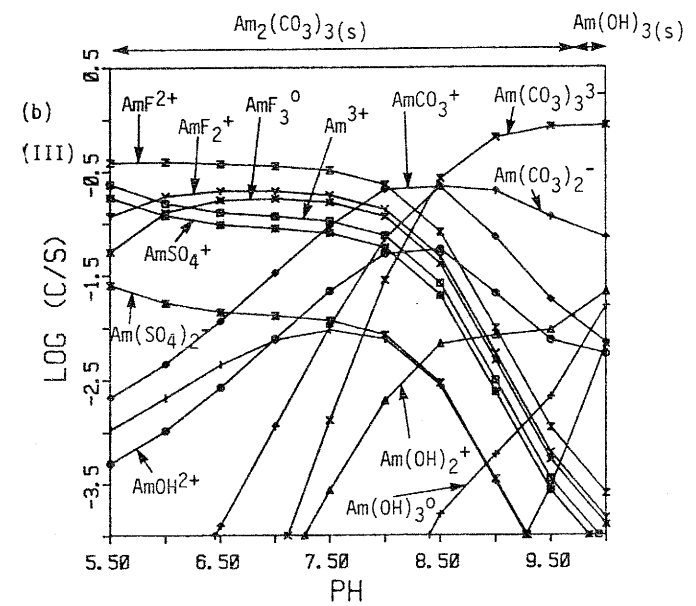
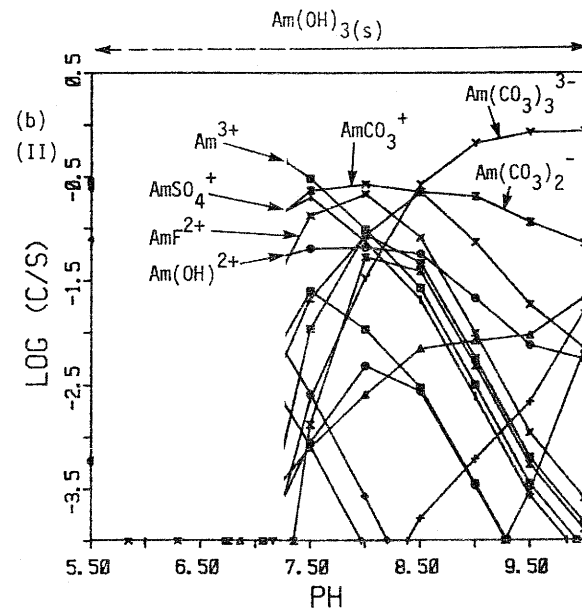
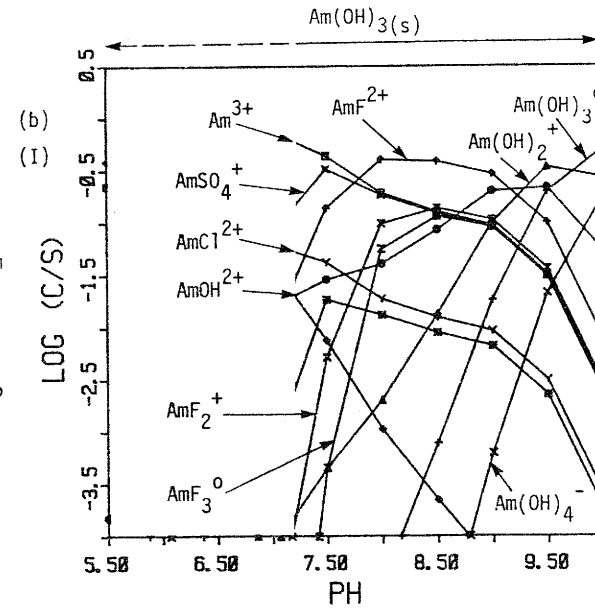
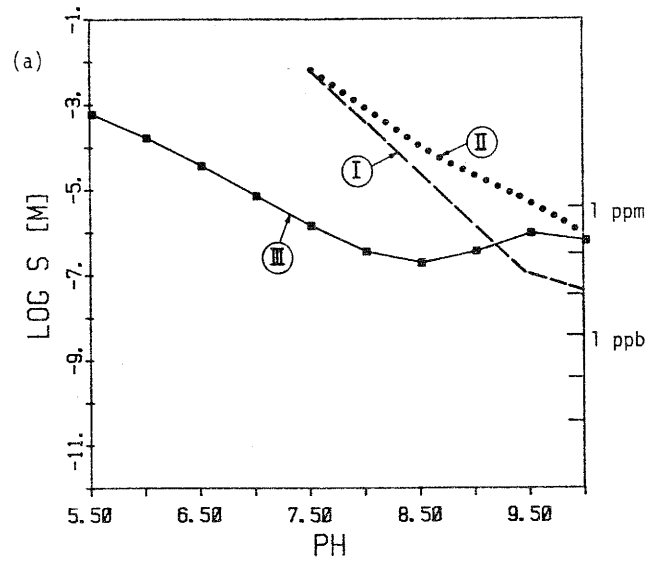


Figure 18.

4. SUMMARY AND CONCLUSIONS

The primary objectives of the present study are :

- an analysis of the importance of various factors which might affect actinide solubility and speciation in natural groundwaters;
- the indication of reasonably conservative actinide solubility limits for subsequent use in geospheric radionuclide transport models in the context of safety assessment.

These tasks are tackled by means of a mathematical speciation model based on a chemical equilibrium concept (Appendix B). The model operated under following restrictions :

- dissolved actinide species considered are limited to low-molecular weight complexes formed with a few inorganic ligands deemed to be important (hydroxide, fluoride, phosphate, carbonate, chloride); interaction with organic ligands or colloid formation were neglected.
- conversion of complex formation constants in the temperature interval 25 to 75 C with a simple van't Hoff approximation.
- correction of mass action law constants with Davies' approximation within ionic strength interval 0 to 0.5.

A series of assumptions were made to favour an overestimation of effective actinide solubilities within the limits of the above model :

- only actinide oxides or hydroxides accepted as potential solubility-limiting phases.
- definition of a reference water with relatively high actinide complexation capacity (expressed by total concentrations of inorganic ligands at, or slightly above, maximum values observed in groundwaters (Table 3) and omission of competing cations) and with ionic strength fixed at a fairly high level (0.2).

Reference calculations were performed for Th, U, Np, Pu and Am at 25 C with two alternative thermodynamic databases (Appendix A), which have been derived from different compilations. The first one is based on extended element-specific reviews of various authors, the second exclusively includes data used for speciation modelling within the framework of KBS-3 (1983). Solubility isopleths, limiting solids and dominant dissolved species are presented graphically as functions of Eh and pH

within preset ranges (from -400 to 700 mV and 5.5 to 10, respectively). From these diagrams we may infer :

- The differences between the two databases are directly reflected in the results since stability constants are inconsistent for important dissolved and solid species.

- The tetravalent oxides $MO_2(s)$ turn out to be the critical solid phase in a large part of the Eh/pH domain considered for the multivalent actinides (U, Np, Pu) and Th.

- Carbonate, fluoride, phosphate and, to a lesser extent, sulphate may be important ligands for stabilizing dissolved actinides under the conditions considered (i.e. water composition, pH and Eh ranges).

The sensitivity of actinide solubility and speciation results was checked with respect to a few model parameters :

- Whenever sufficient enthalpy data were available to establish formation constant databases at 75 C, comparative runs were performed for 25 and 75 C. In these cases, the solubilities for Th, U and Pu are shifted by -2, +2 and -2 orders of magnitude, respectively, when temperature increases from 25 to 75 C. These differences are of the order of the uncertainties associated with many of the formation constants at 25 C (see e.g. Fig. 3).

- Ionic strength effects were investigated by two comparative case studies for U (Figs. 7 and 8). The model predicts solubility enhancement with ionic strength increasing from 0 to 0.2. The differences are, again, not very important when compared with formation constant uncertainties, except in cases where high-charged species are predicted to dominate in solution (such as $UO_2(CO_3)_4$, $NpO_2(CO_3)_3$, $(UO_2)_3(CO_3)_6$). The application of Davies' formula to estimate the activity coefficients of such species is not justified, but tends to shift calculated solubility in a conservative direction.

Additional plots depict actinide speciation and solubility for three fixed linear Eh/pH relationships, which are assumed to characterize lower and upper redox potential boundaries for reducing environments and typical oxygenated waters, respectively. Such solubility curves were used to evaluate the model predictions in the light of a 'reasonable' overestimation of literature data on dissolved actinide concentrations in appropriate aqueous systems. More sophisticated model tests are, in general, constrained by poor characterization of pertinent redox conditions. The evaluations nevertheless allow selection of the 'better' database and speculation about the relative degree of conservatism of the predictions.

Validated maximum solubility diagrams could serve as input for geospheric nuclide migration models, requiring the definition of in-situ pH and Eh (either given precisely or as interval). Detailed information about temperature and water chemistry would not be necessary as long as these parameters lie within the limits of the model. As an example, the curves given in Fig. 19 represent proposed upper concentration limits in reducing groundwater environments (such as expected for undisturbed deep granitic waters). Their selection and reliability has been discussed in Section 3. They could be applied to models of the repository far-field where reducing conditions should prevail. Similar plots are possible for the near-field zone provided reasonable Eh/pH characteristics can be defined. It has been postulated (e.g. Neretnieks (1982)) that a net oxidizing zone will exist around a repository due to water radiolysis with subsequent loss of the fairly unreactive hydrogen gas by diffusion. A theoretical study on the geochemistry of the repository near-field has been initiated at EIR (McKinley et al. (1983b)).

Figure 19 deserves additional discussion. The right-hand side of the diagram displays ranges for maximum actinide solubility as stated in KBS-3 (1983). These values, apparently, have been constructed by adding a 'safety increment' (roughly one order of magnitude) to the maximum solubilities Allard (1983) calculated within pH range 7 to 9 for 25 C. The present approach is different in applying the 'safety margin' not to the overall result but to individual model parameters. Our curves lie, for pH interval 7 to 9, within or above the ranges used in KBS-3, with the exception of Pu. The Pu concentration limit at pH 7 agrees, however, with KBS-3. The differences are, to some extent, caused by the use of a thermodynamic dataset which is not identical to Allard's (1983) base (Th, U). Additionally, Allard (1983) neglected actinide complex formation with ligands other than hydroxide and carbonate ions. Further, he did not correct for ionic strength effects, worked with an empirical free carbonate/pH relationship (instead of an empirical total carbonate/pH function) and accepted carbonates as limiting solids.

From the point of view of model validation, it is probably correct to consider the curves given for U and Th in Fig. 19 as reasonably conservative (consult Figs. 5 and 10). The curve for Am is, probably, too pessimistic since the reference solution turned out to be oversaturated with respect to $\text{Am}_2(\text{CO}_3)_3$ (s). Inclusion of this solid phase leads to a considerable reduction of Am solubility (Fig. 18), and the corresponding curve could be used if its conservatism can be evaluated. The degree of conservatism for the Np and Pu curves cannot be judged as required solubility data are lacking for reducing solutions (in fact, the choice between the two datasets was based on the model predictions for oxic conditions). The Pu curve seems particularly uncertain: all experimental Pu concentrations depicted

in Fig. 17 exceed the limits both datasets propose for aerated waters. At the present stage, the upper concentration limits given for Pu and Np in Fig. 19 should be considered as rough estimates only.

It should be pointed out clearly that the calculations performed in this report cannot yield guaranteed information applicable to define actinide mobility in groundwater systems. This work should rather be considered as a first step in the definition of solubility restrictions for actinides under expected conditions. The following major sources of uncertainty must be reduced or eliminated in order to obtain any significant improvement in quality of output data :

(a) theoretical background

The fundamental assumption of an overall equilibrium between the included chemical components may be invalid due to kinetic hindrance of important processes. Typical examples are the formation of metastable precipitates from oversaturated solutions or the (common) formal existence of individual 'Eh' values for various redox couples which do not correspond to an 'Eh' value measured with a Pt electrode. The extent to which equilibrium models can be applied to real geochemical systems must be clarified, although the relevant time scales are large.

Extrapolation of formation constants from their reference state to other temperatures and ionic strengths involves crude assumptions which should be checked experimentally for important data.

Consideration of actinide complexes with a few inorganic ligands only is obviously simplistic as dissolved organic substances in particular (as present in surface waters) are expected to have significant impact on actinide solubility. This has been examined by Langmuir and Herman (1980) for Th and oxalic acid. Very few background data for such complexes are available, however, and greater emphasis on the laboratory studies necessary to provide such information is required.

Present models are generally limited to low-molecular weight species in solution and thus transportable actinide colloids (true colloids or actinides sorbed on carrier colloids) are not considered. Development of the basic model to include such factors would greatly enhance its applicability.

(b) quality of thermodynamic data

Solids and dissolved species of actinides are characterized by crude, sometimes inconsistent and incomplete thermodynamic data. Variations in values for important species both reported and used in the literature can vary by several orders of magnitude. The poor quality of the overall thermodynamic data sets used is an inherent constraint on reliability and a large experimental effort to produce more reliable data, particularly for Np and Pu, is required. Further basic research on topics such as metastable solid phases or solid solutions would help to establish relevant chemical boundary conditions.

(c) model validation

Literature data for dissolved Pu, Np or Am under reducing geospheric conditions are virtually absent although they are essential to 'tune' the model.

Generally, insufficient characterization of environmental or experimental conditions (e.g. redox conditions) minimizes the usefulness of data reported.

A conclusive model validation on the basis of natural waters is difficult since such solutions are frequently far away from saturation with respect to transuranics (dilution effect). A critical evaluation requires the identification and characterization of locations with potentially high saturation levels.

Problems inherent to the extrapolation of laboratory experiments to field conditions (e.g. time scale) are shared with most other waste management fields. In addition, many experiments suffer from analytical difficulties (e.g. sorption on vessels, filtration, centrifugation) which render much current data questionable. The possible use of natural analogues to examine such effects should be investigated.

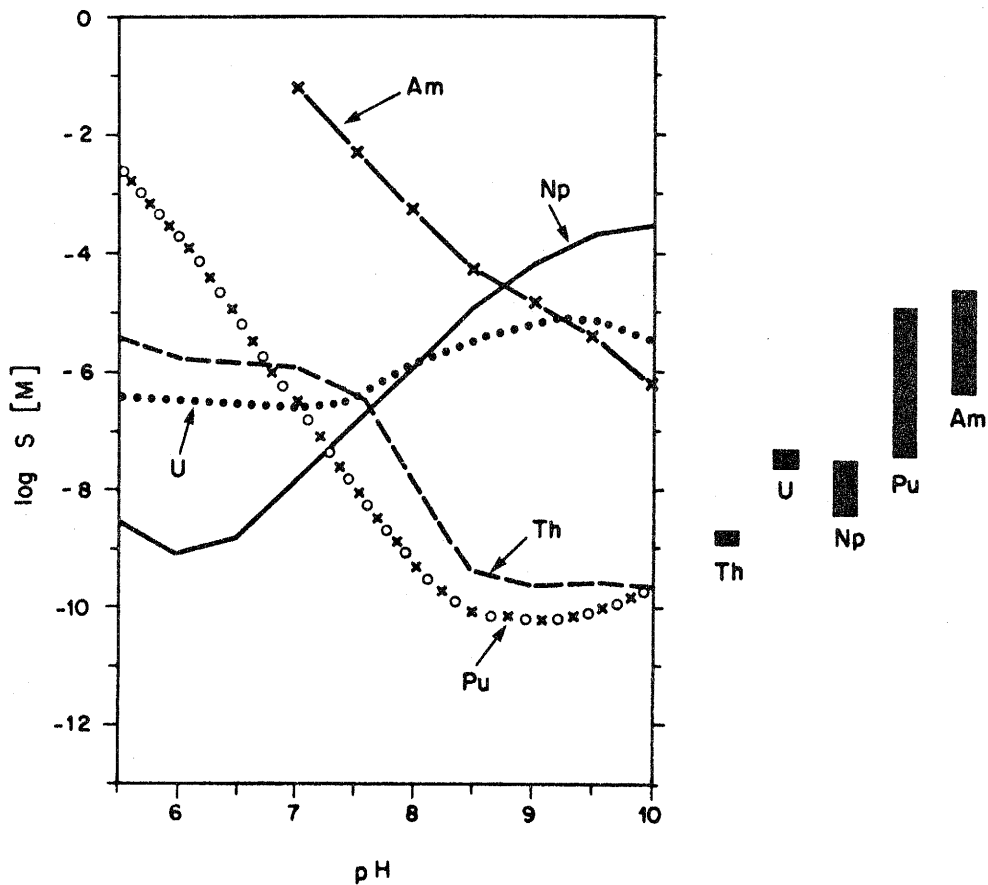
Figure 19: Proposed estimates for upper actinide solubility limits in reducing groundwaters as a function of pH. Temperature range from 25 to 75 C, redox potential range

$$220 - 59 \text{ pH} \leq \text{Eh(mV)} \leq 407 - 59 \text{ pH} ,$$

only actinide oxides or hydroxides as solubility-limiting phases.

The curves for Th and U are considered as 'reasonably' conservative. The conservatism of the Np and, especially, the Pu curve has not been demonstrated. Maximum Am solubility is considerably lowered if its carbonate solid is accepted as potential limiting phase.

Bars define solubility ranges given for pH interval 7 to 9 in the most recent Swedish safety report on the final storage of spent fuel (KBS-3 (1983), Table 12-8).



5. REFERENCES

Allard B. (1982) Solubilities of Actinides in Neutral or Basic Solutions. In: Edelstein N.M. [ed.] "Actinides in Perspective". Pergamon Press, 553-580.

--- (1983) Actinide solution equilibria and solubilities in geologic environments. KBS Technical Report 83-35.

Andelman J.B., Rozzell T.C. (1970) Plutonium in the water environment. 1. Characteristics of aqueous Plutonium. In: 'Radionuclides in the Environment', ACS Advances in Chemistry Series 93: 118-138.

Asikainen M., Kahlos H. (1979) Anomalously high concentrations of uranium, radium and radon in waters from drilled wells in the Helsinki region. Geochim. Cosmochim. Acta 43: 1681-1686.

Baes C.F. Jr., Mesmer R.E. (1976) 'The Hydrolysis of Cations'. Wiley Interscience, New York.

Bischoff K. (1982) private communication.

Cleveland J.M., Rees T.F., Nash K.L. (1983a) Neptunium and Americium speciation in selected Basalt, Granite, Shale and Tuff ground waters. Science 221: 271-273.

---, ---, --- (1983b) Plutonium speciation in selected basalt, granite, shale and tuff groundwaters. Nucl. Technol. 62: 298-310.

Cotton A.F., Wilkinson G. (1970) 'Anorganische Chemie'. Verlag Chemie Weinheim, 1007 pp.

DeRegge P., Bonne A., Huys D., Heremans R. (1979) Experimental investigation of the behaviour of long-living radioisotopes in a natural water-clay system. Proc. OECD/NEA Workshop on the Migration of Long-lived Radionuclides in the Geosphere, Brussels, January 1979, 87-100.

Eisenbud M., Lei W., Ballard R., Krauskopf K., Penna Franca E., Cullen T.L., Freeborn P. (1982) Mobility of Thorium from the Morro del Ferro. Proc. IAEA Symposium on Environmental Migration of Long-Lived Radionuclides, Knoxville, 27-31 July 1981, 739-755.

Goodwin B. (1980) Maximum total uranium solubility under conditions expected in a nuclear waste vault. AECL Technical Report 29.

--- (1982) Calculated uranium solubility in groundwater : implications for nuclear fuel waste disposal. Can. J. Chem. 60: 1759-1766.

KBS-3 (1983) Final Storage of Spent Nuclear Fuel - III. Barriers. SKBF/KBS Safety Report.

Kortuem G. (1966) 'Einfuehrung in die chemische Thermodynamik'. Verlag Chemie Weinheim, 349pp.

Langmuir D., Herman J.S. (1980) The mobility of Thorium in natural waters at low temperatures. Geochim. Cosmochim. Acta 44: 1753-1766.

Laurent S. (1983) Analysis of groundwaters from deep boreholes in Fjaellveden. KBS Technical Report 83-19.

Lemire R.J., Tremaine P.R. (1980) Uranium and Plutonium equilibria in aqueous solutions to 200 C. J. Chem. Eng. Data 25: 361-370.

McKinley I.G., Schweingruber M. (1983a) An assessment of basic thermodynamic data for tetravalent actinide dioxides. EIR internal report TM-45-83-31.

---. ---, Hadermann J. (1983b) Work in progress.

NAGRA (1980) Projektstudie fuer die Endlagerung von hoch-aktiven Abfaellen in tiefliegenden geologischen Formationen sowie fuer die Zwischenlagerung. NAGRA Technical Report NTB-80-02.

--- (1981) Hydrogeologisches Untersuchungsprogramm Nord-schweiz : chemische und physikalische Wasseruntersuchungen. (data collection started in 1981).

Neretnieks I. (1982) The movement of a redox front downstream from a repository for nuclear waste. KBS Technical Report 82-16.

Nishita H. (1979) A Review of Behaviour of Plutonium in Soils and Other Geologic Material. U.S. Nuclear Regulatory Commission Report NUREG/CR-1056.

Olofsson U., Allard B. (1983a) Complexes of actinides with naturally occurring organic substances - Literature survey. KBS Technical Report 83-09.

---, ---, Bengtsson M., Torstenfelt B., Andersson K. (1983b) Formation and properties of actinide colloids. KBS Technical Report 83-08.

Osmond J.K., Cowart J.B. (1976) The theory and use of natural uranium isotopic variations in hydrology. Atomic Energy Review 14: 621-674.

Phillips S.L. (1982) Hydrolysis and formation constants. LBL-14313.

Rai D., Serne R.J., Moore D.A. (1977) Identification of Plutonium compounds and their solubility in soils. Waste Isolation Safety Assessment Program, Task 4, PNL-SA-6957, 107-123.

---, --- (1978) Solid phases and solution species of different elements in geologic environments. PNL-2651.

---, Strickert R.G., McVay G.L. (1982) Neptunium concentration in solution contacting actinide doped glass. Nucl. Technol. 58: 69-76.

Sato M. (1960) Oxidation of sulfide ore bodies. 1. Geochemical environments in terms of Eh and pH. Econ. Geol. 55: 928-961.

Schweingruber M. (1981) Loeslichkeits- und Speziationsberechnungen fuer U, Np, Pu und Th in natuerlichen Grundwaessern - Theorie, thermodynamische Dateien und erste Anwendungen. EIR Report No 449.

--- (1982a) Evaluation of solubility and speciation of actinides in natural groundwaters. In: Lutze W. [ed.] "Scientific Basis for Radioactive Waste Management V". North Holland, 679-688.

--- (1982b) User's Guide for Extended MINEQL (EIR version) - Standard Subroutine / Data Library Package. EIR Internal Report TM-45-82-38.

---, McKinley I.G. (1983) Evaluation of pH, Eh and carbonate data obtained within the regional NAGRA well water sampling programme for northern Switzerland. EIR Internal Report TM-45-83-38.

Skytte Jensen B. (1982) 'Migration phenomena of radionuclides into the geosphere'. Radioactive Waste Monograph Vol. 5, Harwood Acad. Publishers.

Stumm W., Morgan J.J. (1970) "Aquatic Chemistry". Wiley Interscience.

Susak N.J., Friedman A., Fried S., Sullivan J.C. (1983) The reduction of Np(VI) by basalt and olivine. Nucl. Technol. 63: 266-270.

Truesdell A.H., Jones B.F. (1974) WATEQ - A computer program for calculating chemical equilibria of natural waters. Jour. Research U.S. Geol. Survey 2: 233-248.

Westall J.C., Zachary J.L., Morel F.M.M. (1976) MINEQL - A computer program for the calculation of chemical equilibrium composition of aqueous systems. MIT Technical Note 18.

APPENDIX A: THERMODYNAMIC DATA

Table	Topic	page

	Comments	a-1
A-1	References	a-2
A-2	Ligand protonation	
	A-2-1 log K	a-3
	A-2-2 Delta H ₀	a-3
A-3	Actinide redox equilibria	
	A-3-1 log K	a-4
	A-3-2 Delta H ₀	a-4
A-4	Trivalent actinide complexes	
	A-4-1 log K	a-5
	A-4-2 Delta H ₀	a-7
A-5	Tetravalent actinide complexes	
	A-5-1 log K	a-8
	A-5-2 Delta H ₀	a-10
A-6	Pentavalent actinide complexes	
	A-6-1 log K	a-11
	A-6-2 Delta H ₀	a-12
A-7	Hexavalent actinide complexes	
	A-7-1 log K	a-13
	A-7-2 Delta H ₀	a-15

Comments

Tables A-2 to A-7 list thermodynamic data on the formation of dissolved species, solid phases (subscript (s)) and gases (subscript (g)), as defined by the reaction associated with each table and as used in computational work for the present report.

Reported are reaction constants, $\log K$, and reaction enthalpies, ΔH_0 , for 25 C, 1 atm and $I=0$. Reaction constants reported for I deviating from 0 were extrapolated to $I=0$ with Davies' approximation for single ion activity coefficients. Enthalpies are given in kcal/mol; for conversion into kJ/mol, multiply with factor 4.186.

The numerical values are referenced by lower-case letters to identify the sources given in Table A-1. The assignment to one of the alternative 'working' databases, A or B, is displayed by column 'db'. Note that bracketed values are certainly recognized as tentative (guesses, extrapolated values).

If $\log K$ values are lacking, species are considered to be 'non-existent'. Unspecified ΔH_0 values for 'existing' species are set to zero during computations.

Database A relies on recent compilations of thermochemical characteristics for individual actinides, omitting newer data given by Allard. Primary sources are: Lemire and Tremaine for U and Pu (ref. e), Langmuir for Th and U (refs. h and i), Phillips for Am (ref. l). Occasionally, these data are supplemented by information taken from other sources. Np data are collected from a variety of sources including KBS report 55 (ref. b).

Database B exclusively comprises data proposed by Allard. Data for actinide hydrolysis and carbonate complexes are taken from his most recent report (ref. g), and his estimates for the formation constants of the various oxidation states of an 'average' actinide ('An') are accepted for fluoride, phosphate and sulphate complexes (ref. a). No ΔH_0 values are available. Note that U(III) and Np(III) complexes are neglected in ref. g.

Ligand protonation data (Table A-2) are taken from Smith and Martell (ref. c) with a few ΔH_0 values added as derived from thermochemical data presented by Lemire and Tremaine (ref. e). These are used in both datasets.

Table A-1. References.

-
- a Allard B. (1982) in : Edelstein N.M. [Ed], "Actinides in Perspective", Proc. Actinide 1981 Conference, Pacific Grove, CA, Sept. 10-15, 1981, Pergamon.
 - b Allard B., Kipatsi H., Rydberg J. (1977) KBS Technical Report 55.
 - c Smith R.M., Martell A.E. (1976) "Critical Stability Constants", Plenum Press.
 - d Pourbaix M. (1974) "Atlas of electrochemical equilibria in aqueous systems", NACE / CEBELCOR, Brussels.
 - e Lemire R.J., Tremaine P.R. (1980) J. Chem. Eng. Data 25: 361-370.
 - f Skytte Jensen B. (1982) "Migration phenomena of radionuclides into the geosphere". CEC Radioactive Waste Management Series of Monographs, Harwood Acad. Publishers, Vol 5.
 - g Allard B. (1983) Actinide solution equilibria and solubilities in geologic systems. KBS Technical Report 83-35.
 - h Langmuir D., Herman J.S. (1980) Geochim. Cosmochim. Acta 44: 1753-1766.
 - i Langmuir D. (1978) Geochim. Cosmochim. Acta 42: 547-569.
 - j Baes C.F., Mesmer R.E. (1976) "The hydrolysis of cations", John Wiley N.Y. .
 - k Rai D., Serne R.J. (1978) PNL-2651 / UC-70, Pacific Northwest Lab.
 - l Phillips S.L. (1982) LBL-14313 / UC-70, Lawrence Berkeley Lab.

Table A-2. Ligand protonation.

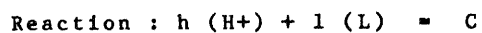


Table A-2-1. log K (25 C, 1 atm, I=0)

C / L	OH-	CO3-2	F-	PO4-3	SO4-2	db
(H)(L)	14.00 c	10.33 c	3.17 c	12.35 c	2.00 c	A=B
(H)2(L)	---	16.68 c	---	19.55 c	---	A=B
(H)3(L)	---	---	---	21.70 c	---	A=B
(H)2(L) (g)	---	18.14 c	---	---	---	A=B

Table A-2-2. Delta HO (25 C, 1 atm, I=0) [kcal/mol]

C / L	OH-	CO3-2	F-	PO4-3	SO4-2	db
(H)(L)	-13.34 c	-3.5 c	3.2 c	-3.5 c	5.4 c	A=B
(H)2(L)	---	-5.5 c	---	-4.3 c	---	A=B
(H)3(L)	---	---	---	-2.42 e	---	A=B
(H)2(L) (g)	---	-0.51 e	---	---	---	A=B

Table A-3. Actinide redox equilibria.

Table A-3-1. log K (25 C, 1 atm, I=0) @

Reaction / M	U	Pu	Np	db
M ⁴⁺ + e ⁻ = M ³⁺	-8.8 e	16.9 e	2.6 d	A
	-8.8 g	17.05 g	2.5 g	B
MO ₂ ⁺ + e ⁻ + 4 H ⁺ = M ⁴⁺ + 2 H ₂ O	6.4 e	18.6 e	12.7 d	A
	7.8 g	18.6 g	11.0 g	B
MO ₂ ²⁺ + e ⁻ = MO ₂ ⁺	2.8 e	16.3 e	19.4 d	A
	1.35 g	16.2 g	20.8 g	B

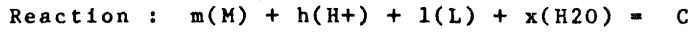
@ equal to $E_0[\text{mV}]/59.16$, where E_0 = standard electrode potential versus standard hydrogen electrode (SHE) at 25 C, 1 atm, I=0.

Table A-3-2. Delta H₀ (25 C, 1 atm, I=0) [kcal/mol] §

Reaction / M	U	Pu	Np	db
M ⁴⁺ + e ⁻ = M ³⁺	24.4 e	-13.3 e	---	A
	---	---	---	B
MO ₂ ⁺ + e ⁻ + 4 H ⁺ = M ⁴⁺ + 2 H ₂ O	-31.2 e	-46.2 e	---	A
	---	---	---	B
MO ₂ ²⁺ + e ⁻ = MO ₂ ⁺	-3.3 e	-22.2 e	---	A
	---	---	---	B

§ computed by substitution of $(e^-) = .5 * H_2(g) - (H^+)$, with $\Delta G_0^f = 0$ and $S_0 = 31.21 \text{ cal/mol deg}$ for $H_2(g)$ (from ref. i).

Table A-4. Complex formation of trivalent actinides.



with $L = (CO_3^{2-}), (F^-), (Cl^-), (SO_4^{2-}), (PO_4^{3-})$.

Table A-4-1. log K (25 C, 1 atm, I=0)

C / M	An+3	U+3	Pu+3	Np+3	Am+3	db
M(OH)	---	(-7.0) b	-7.0 c	-7.0 b	(-8.0) l	A
	-8.0 a	---	(-7.5) g	---	-7.5 g	B
M(OH)2	---	(-14.0) b	(-15.0) b	(-15.0) b	(-16.9) l	A
	-17.0 a	---	(-16.5) g	---	-16.5 g	B
M(OH)3	---	(-23.0) b	(-26.0) b	(-25.0) b	(-26.5) l	A
	-26.5 a	---	(-26.5) g	---	(-26.5) g	B
M(OH)4	---	(-33.0) b	(-33.0) b	(-35.0) b	(-37.1) l	A
	-37.0 a	---	(-37.0) g	---	(-37.0) g	B
(M)2(OH)2	---	(-14.7) b	---	(-14.0) b	(-13.9) l	A
	-14.0 a	---	(-14.0) g	---	(-14.0) g	B
(M)3(OH)5	---	(-32.0) b	---	(-32.0) b	---	A
	-33.0 a	---	(-33.0) g	---	(-33.0) g	B
M(OH)3 (s)	---	-22.7 d	-22.3 e	(-22.) d	(-18.7) j	A
	-18.5 a	---	(-18.5) g	---	(-18.5) g	B
(M)2(O)3 (s)	---	---	-48.1 e	---	---	A
	---	---	---	---	---	B
M(CO3)	---	(9.6) f	(9.6) f	(9.6) f	---	A
	6.5 a	---	(6.0) g	---	6.0 g	B
M(CO3)2	---	(12.9) f	(12.9) f	(12.9) f	---	A
	11.0 a	---	(10.0) g	---	10.0 g	B
M(CO3)3	---	(16.2) f	(16.2) f	(16.2) f	---	A
	14.5 a	---	(13.0) g	---	(13.0) g	B
M(OH)(CO3)2	---	---	---	---	---	A
	(-1.5) a	---	---	---	---	B
(M)2(CO3)3 (s)	---	---	---	---	---	A
	31.0 a	---	(31.0) g	---	31.0 g	B
M(F)	---	---	---	---	4.3 l	A
	4.3 a	---	(4.3) a	---	(4.3) a	B
M(F)2	---	---	---	---	7.4 l	A
	7.6 a	---	(7.6) a	---	(7.6) a	B
M(F)3	---	---	---	---	10.6 l	A
	10.8 a	---	(10.8) a	---	(10.8) a	B

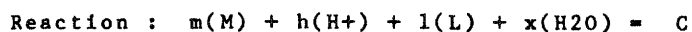
Table A-4-1. log K (25 C, 1 atm, I=0) (continued)

C / M	An+3	U+3	Pu+3	Np+3	Am+3	db
M(F)3 (s)	--- 10.2 a	---	10.0 e (10.2) a	---	--- (10.2) a	A B
M(Cl)	---	---	0.8 c	---	1.1 1	A
M(Cl)2	---	---	---	---	---	B A B
M(Cl)3 (s)	---	---	11.4 k	---	---	A B
M(SO4)	---	---	3.1 c	---	3.6 1	A
M(SO4)2	3.5 a	---	(3.5) a	---	(3.5) a	B
M(HSO4)2	5.2 a	---	(5.2) a	---	5.0 1 (5.2) a	A B
M(HPO4)	---	---	---	---	---	A B
M(H2PO4)	(18.3) a	---	(18.3) a	---	(18.3) a	A
M(H2PO4)2	22.0 a	---	22.0 e (22.0) a	---	22.2 1 (22.0) a	A B
M(PO4) (s)	---	---	---	---	42.8 1 ---	A B
M(PO4) (s)	23.0 a	---	(23.0) a	---	(23.0) a	A B

Table A-4-2. Delta H₀ (25 C, 1 atm, I=0) [kcal/mol]

C / M	An+3	U+3	Pu+3	Np+3	Am+3	db
M(OH)	---	---	12.8 e	---	---	A
M(OH) ₂	---	---	---	---	---	A
M(OH) ₃	---	---	---	---	---	A
M(OH) ₄	---	---	---	---	---	A
(M) ₂ (OH) ₂	---	---	---	---	---	A
(M) ₃ (OH) ₅	---	---	---	---	---	A
M(OH) ₃ (s)	---	---	35.5 e	---	---	A
(M) ₂ (O) ₃ (s)	---	---	86.1 e	---	---	A
M(CO ₃)	---	---	---	---	---	A
M(CO ₃) ₂	---	---	---	---	---	A
M(CO ₃) ₃	---	---	---	---	---	A
M(OH)(CO ₃) ₂	---	---	---	---	---	A
(M) ₂ (CO ₃) ₃ (s)	---	---	---	---	---	A
M(F)	---	---	---	---	---	A
M(F) ₂	---	---	---	---	---	A
M(F) ₃	---	---	---	---	---	A
M(F) ₃ (s)	---	---	11.1 e	---	---	A
M(Cl)	---	---	---	---	---	A
M(Cl) ₂	---	---	---	---	---	A
M(Cl) ₃ (s)	---	---	---	---	---	A
M(SO ₄)	---	---	3.5 e	---	---	A
M(SO ₄) ₂	---	---	---	---	---	A
M(HSO ₄) ₂	---	---	---	---	---	A
M(HPO ₄)	---	---	---	---	---	A
M(H ₂ PO ₄)	---	---	3.5 e	---	---	A
M(H ₂ PO ₄) ₂	---	---	---	---	---	A
M(PO ₄) (s)	---	---	---	---	---	A

Table A-5. Complex formation of tetravalent actinides.



with $L = (CO_3-2), (F-), (Cl-), (SO_4-2), (PO_4-3)$

Table A-5-1. log K (25 C, 1 atm, I=0)

C / M	An+4	Th+4	U+4	Pu+4	Np+4		db
M(OH)	---	-3.2 h	-0.65 i	-0.7 e	-1.5 b		A
	-0.5 a	-3.2 g	-0.6 g	-0.5 g	-1.5 g		B
M(OH)2	---	-6.95 h	(-2.25)i	(-2.3) e	(-4.0) b		A
	-2.5 a	-6.9 g	-2.5 g	-2.5 g	-3. g		B
M(OH)3	---	(-11.7) h	(-4.9)i	(-5.3) e	(-8.0) b		A
	-6.0 a	-11.7 g	-5.5 g	-5.5 g	-6.0 g		B
M(OH)4	---	-15.9 h	(-8.5) i	(-9.5) e	(-13.0) b		A
	-10.5 a	-15.9 g	-10. g	-9.5 g	-10. g		B
M(OH)5	---	---	(-13.15)i	(-15.0) e	(-20.0) b		A
	-20.0 a	---	(-19.) g	(-19.) g	(-20.) g		B
(M)2(OH)2	---	(-6.1) h	---	---	---		A
	-1.0 a	---	(-1.) g	(-1.) g	(-2.) g		B
(M)4(OH)8	---	(-21.1) h	---	---	---		A
	(-2.0) a	---	---	---	---		B
(M)6(OH)15	---	(-36.7) h	-17.2 j	---	---		A
	(0.0) a	---	---	---	---		B
M(OH)4 (s)	---	-11.3 c	-9.8 k	(-1.0) e	-0.8 k		A
	---	---	---	---	---		B
M(O)2 (s)	---	-6.3 h	4.6 e	7.0 e	2.7 k		A
	-2.0 a	-6.3 g	0.6 g	1. g	0. g		B
(M)4(O)9 (s) §	---	---	16.3 e	---	---		A
	---	---	---	---	---		B
M(CO3)	---	11.0 l	---	---	---		A
	---	---	---	---	---		B
M(CO3)5	---	---	---	---	---		A
	(37.) a	---	36.5 g	(36.5) g	(36.5) g		B
M(OH)3(CO3)	---	---	(-1.0) f	(-1.0) f	(-1.0) f		A
	(0.) a	---	(0.) g	(0.) g	(0.) g		B
M(F)	---	8.0 h	8.6 i	7.9 e	(8.3) c		A
	8.6 a	(8.6) a	(8.6) a	(8.6) a	(8.6) a		B
M(F)2	---	14.2 h	14.5 i	---	(14.5) c		A
	14.5 a	(14.5) a	(14.5) a	(14.5) a	(14.5) a		B
M(F)3	---	18.9 h	19.1 i	---	(20.3) c		A
	19.1 a	(19.1) a	(19.1) a	(19.1) a	(19.1) a		B
M(F)4	---	22.3 h	23.5 i	---	(25.1) c		A
	23.6 a	(23.6) a	(23.6) a	(23.6) a	(23.6) a		B

Table A-5-1. log K (25 C, 1 atm, I=0) (continued)

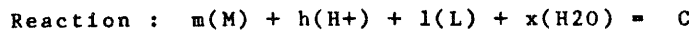
C / M	An+4	Th+4	U+4	Pu+4	Np+4	db
M(F)5	--- 25.3 a	--- (25.3) a	25.2 i (25.3) a	--- (25.3) a	--- (25.3) a	A B
M(F)6	--- ---	--- ---	27.7 i ---	--- ---	--- ---	A B
M(F)4 (s)	--- 24.0 a	30.1 h (24.0) a	18.5 i (24.0) a	(13.0) e (24.0) a	--- (24.0) a	A B
M(Cl)	--- ---	1.1 h ---	(3.) e ---	0.9 e ---	(1.2) k ---	A B
M(Cl)2	--- ---	0.8 h ---	--- ---	1.9 k ---	(1.9) k ---	A B
M(Cl)3	--- ---	1.65 h ---	--- ---	--- ---	--- ---	A B
M(Cl)4	--- ---	1.26 h ---	--- ---	--- ---	--- ---	A B
M(SO4)	--- 5.6 a	5.45 h (5.6) a	4.7 c (5.6) a	5.8 e (5.6) a	(3.9) k (5.6) a	A B
M(SO4)2	--- 10.3 a	9.75 h (10.3) a	8.0 c (10.3) a	10.2 e (10.3) a	(5.7) k (10.3) a	A B
M(SO4)3	--- ---	10.5 h ---	--- ---	11.5 k ---	--- ---	A B
M(SO4)4	--- ---	8.5 h ---	--- ---	--- ---	--- ---	A B
M(OH)2(SO4) (s)	--- ---	--- ---	3.2 k ---	--- ---	--- ---	A B
M(HPO4)	--- 25.4 a	25.55 h (25.4) a	24.3 i (25.4) a	25.9 e (25.4) a	--- (25.4) a	A B
M(HPO4)2	--- 48.5 a	51.1 h (48.5) a	46.7 i (48.5) a	49.0 e (48.5) a	--- (48.5) a	A B
M(HPO4)3	--- 70.5 a	72.0 h (70.5) a	67.6 i (70.5) a	70.0 e (70.5) a	--- (70.5) a	A B
M(HPO4)4	--- ---	--- ---	88.0 i ---	92.4 e ---	--- ---	A B
M(H2PO4)	--- 24.1 a	24.1 h (24.1) a	--- (24.1) a	--- (24.1) a	--- (24.1) a	A B
M(H2PO4)2	--- 48.0 a	48.0 h (48.) a	--- (48.) a	--- (48.) a	--- (48.) a	A B
M(H3PO4)	--- ---	23.6 h ---	--- ---	--- ---	--- ---	A B
M(HPO4)2 (s)	--- 51.7 a	51.5 h (51.7) a	51.5 i (51.7) a	52.7 e (51.7) a	--- (51.7) a	A B

§ reaction : 2 (M+4) + 2 (MO2+) + 5 H2O - 10 (H+) = (M)4(O)9 (s)

Table A-5-2. Delta H₀ (25 C, 1atm, I=0) [kcal/mol]

C / M	An+4	Th+4	U+4	Pu+4	Np+4	db
M(OH)	---	(6.0) h	11.8 e	11.5 e	---	A
M(OH)2	---	(13.8) h	17.8 e	17.8 e	---	A
M(OH)3	---	(20.4) h	22.6 e	23.1 e	---	A
M(OH)4	---	(24.7) h	24.8 e	26.1 e	---	A
M(OH)5	---	---	27.6 e	30.1 e	---	A
(M)2(OH)2	---	(14.8) h	---	---	---	A
(M)4(OH)8	---	(57.8) h	---	---	---	A
(M)6(OH)15	---	(108.4) h	---	---	---	A
M(OH)4 (s)	---	(7.5) h	---	16.5 e	---	A
M(O)2 (s)	---	27.2 h	(18.7) e	12.5 e	---	A
(M)4(O)9 (s) \$	---	---	39.8 e	---	---	A
M(CO3)	---	---	---	---	---	A
M(CO3)5	---	---	---	---	---	A
M(OH)3(CO3)	---	---	---	---	---	A
M(F)	---	-1.4 h	5.0 e	5.9 e	---	A
M(F)2	---	-2.1 h	7.2 e	---	---	A
M(F)3	---	-3.0 h	7.2 e	---	---	A
M(F)4	---	-3.8 h	4.5 e	---	---	A
M(F)5	---	---	4.7 e	---	---	A
M(F)6	---	---	3.4 e	---	---	A
M(F)4 (s)	---	2.8 h	12.0 e	23.9 e	---	A
M(Cl)	---	-0.2 h	1.8 e	4.2 e	---	A
M(Cl)2	---	20.9 h	---	---	---	A
M(Cl)3	---	15.8 h	---	---	---	A
M(Cl)4	---	12.3 h	---	---	---	A
M(SO4)	---	3.7 h	1.2 e	3.0 e	---	A
M(SO4)2	---	7.5 h	5.5 e	9.9 e	---	A
M(SO4)3	---	11.7 h	---	---	---	A
M(SO4)4	---	13.1 h	---	---	---	A
M(OH)2(SO4) (s)	---	---	---	---	---	A
M(HPO4)	---	(-3.6) h	7.5 e	6.2 e	---	A
M(HPO4)2	---	(-10.3) h	1.9 e	-0.6 e	---	A
M(HPO4)3	---	-15.7 h	-8. e	-11.7 e	---	A
M(HPO4)4	---	---	-26. e	-31.7 e	---	A
M(H2PO4)	---	12.9 h	---	---	---	A
M(H2PO4)2	---	-3.8 h	---	---	---	A
M(H3PO4)	---	13.7 h	---	---	---	A
M(HPO4)2 (s)	---	(-2.0) h	-3.8 e	1.3 e	---	A

Table A-6. Complex formation of pentavalent actinides.



with $L = (CO_3^{2-}), (F^-), (Cl^-), (SO_4^{2-}), (PO_4^{3-})$

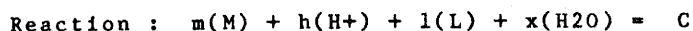
Table A-6-1. log K (25 C, 1 atm, I=0)

C / M	AnO ₂ ⁺	UO ₂ ⁺	PuO ₂ ⁺	NpO ₂ ⁺	db
M(OH)	--- -9.4 a	(-9.4) b (-10.) g	-9.7 e -9.7 g	-9.0 b -8.9 g	A B
M(OH) (s)	--- -5.2 a	(-5.0) f (-5.) g	-5.5 e -5. g	-4.9 k -4.9 g	A B
M(CO ₃)	--- (5.) a	--- (5.) g	--- (5.) g	--- 5.9 g	A B
M(CO ₃) ₂	--- (9.) a	--- (10.) g	--- (10.) g	--- 11.1 g	A B
M(CO ₃) ₃	--- (14.) a	--- (15.3) g	--- (15.3) g	--- 16.3 g	A B
M(HCO ₃)	--- ---	--- ---	--- ---	12.6 k ---	A B
M(HCO ₃) ₂	--- ---	--- ---	--- ---	24.6 l ---	A B
M(F)	--- 3.7 a	--- (3.7) a	--- (3.7) a	--- (3.7) a	A B
M(Cl)	--- ---	--- ---	0.17 k ---	-0.1 k ---	A B
M(SO ₄)	--- 2.0 a	--- (2.) a	--- (2.) a	--- (2.) a	A B
M(HPO ₄)	--- ---	--- ---	--- ---	15.9 k ---	A B

Table A-6-2. Delta H₀ (25 C, 1atm, I=0) [kcal/mol]

C / M	AnO ₂ ⁺	UO ₂ ⁺	PuO ₂ ⁺	NpO ₂ ⁺	db
M(OH)	---	---	16.6 e	---	A
M(OH) (s)	---	---	10.2 e	---	A
M(CO ₃)	---	---	---	---	A
M(CO ₃) ₂	---	---	---	---	A
M(CO ₃) ₃	---	---	---	---	A
M(HCO ₃)	---	---	---	---	A
M(HCO ₃) ₂	---	---	---	---	A
M(F)	---	---	---	---	A
M(Cl)	---	---	---	---	A
M(SO ₄)	---	---	---	---	A
M(HPO ₄)	---	---	---	---	A

Table A-7. Complex formation of hexavalent actinides.



with $L = (CO_3-2), (F-), (Cl-), (SO_4-2), (PO_4-3)$

Table A-7-1. log K (25 C, 1 atm, I=0)

C / M	AnO2+2	UO2+2	PuO2+2	NpO2+2	db
M(OH)	---	-5.8 e	-5.6 e	-5.1 c	A
	-5.7 a	-5.8 g	-5.6 g	-5.1 g	B
M(OH)2	---	(-12.0) e	(-11.0) k	(-11.5) b	A
	-12.0 a	-11.9 g	-10.2 g	-10.4 g	B
M(OH)3	---	(-23.6) k	(-20.7) k	(-20.7) f	A
	---	(-21.) g	(-20.) g	(-19.) g	B
M(OH)4	---	(-37.8) k	---	---	A
	---	---	---	---	B
(M)2(OH)	---	-4.4 c	-4.3 b	(-4.0) b	A
	---	---	---	---	B
(M)2(OH)2	---	-5.6 e	-8.3 e	-6.4 c	A
	-5.5 a	-5.6 g	-8.3 g	-6.4 g	B
(M)3(OH)4	---	-12.2 c	---	---	A
	---	---	---	---	B
(M)3(OH)5	---	-15.5 c	-21.7 e	-17.5 c	A
	-15.5 a	-15.6 g	-21.6 g	(-17.) g	B
M(OH)2 (s)	---	-5.6 e	-3.5 e	-5.3 k	A
	-5.0 a	-5.6 g	-5. g	-5.3 g	B
(M)3(O)8 (s) @	---	1.0 e	---	---	A
	---	---	---	---	B
M(CO3)	---	10.05 e	(13.2) k	(10.0) f	A
	10.0 a	10.1 g	(9.) g	(10.1) g	B
M(CO3)2	---	17.0 e	(14.9) e	(17.0) f	A
	16.7 a	16.7 g	(15.) g	(16.7) g	B
M(CO3)3	---	21.4 e	(20.9) k	(21.0) f	A
	23.8 a	23.8 g	(22.) g	(23.8) g	B
(M)3(CO3)6	---	---	---	---	A
	60.5 a	60.1 g	(60.1) g	(60.1) g	B
M(OH)(CO3)	---	---	(-9.85)k	---	A
	---	---	---	---	B
M(OH)2(CO3)	---	---	(-5.0) k	---	A
	---	---	---	---	B
(M)2(OH)3(CO3)	---	---	---	---	A
	---	-1. g	(-1.) g	(-1.) g	B

Table A-7-1. log K (25 C, 1 atm, I=0) (continued)

C / M	AnO2+2	UO2+2	PuO2+2	NpO2+2	db
(M)3(OH)3(CO3)	--- 4.0 a	--- 1. g	--- (1.) g	--- (1.) g	A B
M(CO3) (s)	--- 13.8 a	14.45 e 13.8 g	14.0 k (13.8) g	--- (13.8) g	A B
M(F)	--- 5.7 a	5.0 e (5.7) a	5.7 e (5.7) a	(4.5) k (5.7) a	A B
M(F)2	--- 11.1 a	8.9 e (11.1) a	11.0 e (11.1) a	(7.8) k (11.1) a	A B
M(F)3	--- 15.9 a	11.5 e (15.9) a	15.8 e (15.9) a	--- (15.9) a	A B
M(F)4	--- 18.8 a	12.6 e (18.8) a	18.7 e (18.8) a	--- (18.8) a	A B
M(Cl)	--- ---	0.2 c ---	0.2 e ---	(0.25)k ---	A B
M(Cl)2	--- ---	--- ---	-0.25 c ---	--- ---	A B
M(SO4)	--- 3.0 a	3.0 c (3.) a	3.0 e (3.) a	3.3 c (3.) a	A B
M(SO4)2	--- 4.3 a	4.0 c (4.3) a	--- (4.3) a	(4.7) c (4.3) a	A B
M(SO4)3	--- ---	(3.7) c ---	--- ---	--- ---	A B
M(HPO4)	--- 20.8 a	(20.5) i (20.8) a	--- (20.8) a	--- (20.8) a	A B
M(HPO4)2	--- 43.2 a	(43.2) i (43.2) a	--- (43.2) a	--- (43.2) a	A B
M(H2PO4)	--- 22.5 a	22.6 i (22.5) a	23.5 e (22.5) a	--- (22.5) a	A B
M(H2PO4)2	--- 44.6 a	44.5 i (44.6) a	--- (44.6) a	--- (44.6) a	A B
M(H2PO4)3	--- ---	65.8 i ---	--- ---	--- ---	A B
M(HPO4) (s)	--- 25.0 a	24.0 i (25.) a	25.4 e (25.) a	--- (25.) a	A B
(M)3(PO4)2 (s)	--- 48.2 a	49.0 i (48.2) a	--- (48.2) a	--- (48.2) a	A B

@ reaction : 2 (MO2+) + (MO2+2) + 2 H2O - 4 (H+) = (M)3(O)8 (s)

Table A-7-2. Delta H0 (25 C, 1 atm, I=0) [kcal/mol]

C / M	AnO2+2	UO2+2	PuO2+2	NpO2+2	db
M(OH)	---	11.0 e	10.8 e	---	A
M(OH)2	---	17.4 e	---	---	A
M(OH)3	---	---	---	---	A
M(OH)4	---	---	---	---	A
(M)2(OH)	---	---	---	---	A
(M)2(OH)2	---	10.1 e	13.8 e	---	A
(M)3(OH)4	---	---	---	---	A
(M)3(OH)5	---	25. e	33.4 e	---	A
M(OH)2 (s)	---	13.6 e	8.6 e	---	A
(M)3(O)8 (s) @	---	19.2 e	---	---	A
M(CO3)	---	-2.8 e	---	---	A
M(CO3)2	---	3.6 e	6.5 e	---	A
M(CO3)3	---	-9.7 e	---	---	A
(M)3(CO3)6	---	---	---	---	A
M(OH)(CO3)	---	---	---	---	A
M(OH)2(CO3)	---	---	---	---	A
(M)2(OH)3(CO3)	---	---	---	---	A
(M)3(OH)3(CO3)	---	---	---	---	A
M(CO3) (s)	---	5.6 e	---	---	A
M(F)	---	-0.6 e	-1.3 e	---	A
M(F)2	---	-0.8 e	-3.7 e	---	A
M(F)3	---	-1.0 e	-7.0 e	---	A
M(F)4	---	-1.0 e	-9.6 e	---	A
M(Cl)	---	0. e	2.8 e	---	A
M(Cl)2	---	---	---	---	A
M(SO4)	---	5.2 e	-1. e	---	A
M(SO4)2	---	---	---	---	A
M(SO4)3	---	---	---	---	A
M(HPO4)	---	-2.0 e	---	---	A
M(HPO4)2	---	-11.5 e	---	---	A
M(H2PO4)	---	-3.5 e	-5. e	---	A
M(H2PO4)2	---	-16.4 e	---	---	A
M(H2PO4)3	---	-28. e	---	---	A
M(HPO4) (s)	---	1.7 e	-1. e	---	A
(M)3(PO4)2 (s)	---	14.4 e	---	---	A

APPENDIX B : MODEL DESCRIPTION

The first section presents the mathematical basis for the actinide speciation calculations in this report. The modelling of temperature, pressure and ionic strength effects for equilibrium constants is treated in the second part.

I. BASIC MODEL

I.1 Definition of upper activity limits for actinide aquo ions

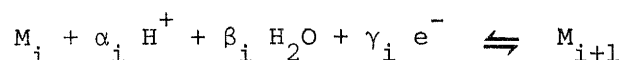
It can be shown that the assumptions of

(a) overall redox equilibrium among the actinide oxidation states and

(b) no oversaturation of the aqueous solution with respect to any pure actinide oxide or hydroxide solid

result in the definition of upper activity limits for actinide aquo ions at fixed pH, redox potential (Eh), pressure (p) and temperature (T).

Let us arrange the aquo ions of n different actinide oxidation states, M_i , in order of decreasing oxidation states. The equilibrium condition between the i-th and (i+1)-th oxidation state may then be expressed by reaction



with the corresponding mass action law (Nernst equation)

$$\frac{Eh \cdot F \cdot \gamma_i}{2.30 \cdot R \cdot T} = \log K_i + \log \frac{\{M_i\}}{\{M_{i+1}\}} - \alpha_i \text{pH} \quad \dots(1)$$

and

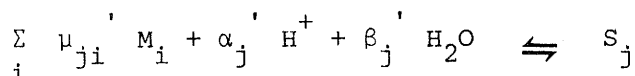
$$\log K_i = \frac{E_i^0 \cdot F \cdot \gamma_i}{2.30 \cdot R \cdot T} \quad \dots(2)$$

coupling the activities of the aquo ions, $\{M_i\}$ and $\{M_{i+1}\}$, with pH and Eh. Greek letters denote stoichiometric coefficients. E_i^0 is the standard potential versus the standard hydrogen electrode (SHE) and K_i is the equilibrium constant for that reaction. Both quantities are dependent on pressure and temperature. R is the gas constant and F the Faraday constant. Note that the activity of water, the solvent, has been set to unity in eq. (1). This is a good approximation for rather

dilute aqueous solutions like the groundwaters to be modelled (see e.g. Truesdell and Jones (1974)) and will be implicitly used along further discussion.

Hence, the condition of redox equilibria among all actinide oxidation states requires a simultaneous validity of eq.(1) for i ranging from 1 to $(n-1)$. For given Eh, pH and E_i^0 we are left with a system of $(n-1)$ independent equations which are linear with respect to the logarithms of the n unknowns, the actinide aquo ion activities.

The lacking equation is supplied by assumption (b). The formation of solid oxide or hydroxide phases can be described by reactions of type



The mathematical criterion for a chemical equilibrium between the solution and one solid, say S_j , with a solid-specific saturation index (SI_j) defined by

$$SI_j = \log K_j' + \sum_i \mu_{ji}' \log \{M_i\} - \alpha_j' \text{pH} \quad \dots(3)$$

is equal to

$$SI_j = 0 \quad \dots(4)$$

The greek symbols in eq.(3) again denote stoichiometric coefficients, and K_j' is called the solubility product.

For a given system of solids with known solubility products, the remaining problem connected with premise (b) is picking out one solid phase S_j such that the solution will not be oversaturated with respect to all other solids. It is solved when

$$SI_j = 0$$

and

...(5)

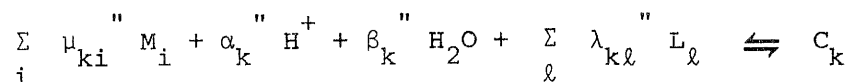
$$SI_j \leq 0 \quad \text{for all } j \neq j.$$

S_j will be called the solubility-limiting solid. The combination of the system of mass action expressions for the redox equilibria (eq. (1)) with the mass action law for the coexistence of the solubility-limiting phase and solution (eq. (3) under condition (5)) defines maximum actinide aquo ion activities, $\{M_i\}_{\max}$, which are compatible with both assumptions (a) and (b), and which will be used below to assess maximum actinide solubility.

In case of a single actinide oxidation state, the limiting aquo ion activity is directly determined by eqs. (3) and (5) and independent of Eh.

I.2 Definition of maximum actinide solubility

Consider a system of formation reactions for dissolved species C_k from a set of components including the actinide aquo ions, the proton, water and some additional components L_ℓ :



At chemical equilibrium, mass action laws of type

$$\{C_k\} = K_k \cdot \prod_i \{M_i\}^{\mu_{ki}} \cdot 10^{-\alpha_k \text{pH}} \cdot \prod_\ell \{L_\ell\}^{\lambda_{k\ell}} \quad \dots(6)$$

will hold for every species. Again, greek letters symbolize stoichiometric coefficients, and K_k is called species formation constant.

We may convert the activities of dissolved species and of all components L_ℓ into concentrations (denoted by $[]$) introducing species-specific activity coefficients f_x ,

$$f_x = \{x\} / [x] \quad \dots(7)$$

and rewrite eq.(6) as

$$[C_k] = Q_k \cdot \prod_\ell [L_\ell]^{\lambda_{k\ell}} \quad \dots(8)$$

where

$$Q_k = K_k \cdot \prod_i \{M_i\}^{\mu_{ki}} \cdot 10^{-\alpha_k \text{pH}} \cdot f_{C_k}^{-1} \cdot \prod_\ell f_{L_\ell}^{\lambda_{k\ell}} \quad \dots(9)$$

Total actinide concentration, $[\Sigma M]$, and total concentration of a component L_ℓ , $[\Sigma L_\ell]$, can be stated as

$$[\Sigma M] = \sum_i \sum_k \mu_{ki} [C_k] \quad \dots(10)$$

and

$$[\Sigma L_\ell] = \sum_k \lambda_{k\ell} [C_k] , \quad \dots(11)$$

respectively.

The system of mass balances (11) can be solved for the free component concentrations $[L_\ell]$ under substitution of eq. (8) with given Q_k . The requirements are from eq. (9): known equilibrium constants and activity coefficients, fixed pH and actinide aquo ion activities. Species concentrations $[C_k]$ can then be computed from eq. (8), total dissolved actinide concentration from eq. (10). The latter is referred to as actinide solubility if the actinide aquo ion activities correspond to the maximum values defined in the section.

The dominant dissolved actinide-carrying species, $C_{\hat{k}}$, is derived from relation

$$[C_{\hat{k}}] \cdot \sum_i \mu_{\hat{k}i} > [C_k] \cdot \sum_i \mu_{ki} \quad \dots(12)$$

for all $k \neq \hat{k}$.

II. AUXILIARY MODELS

II.1 Temperature and pressure dependency of equilibrium constants

The equilibrium constants K (eq. (1)), K' (eq. (3)) and K'' (eq. (6)) are functions of both pressure and temperature.

The conversion of K values from a reference state (p_0, T_0) to state (p, T) can generally be expressed by

$$\log K(p,T) = \log K_{(p_0,T_0)} + \int_{T_0}^T \frac{\Delta H^0(p_0,T_0)dT}{2.30 \cdot R \cdot T^2} - \int_{p_0}^p \frac{\Delta v^0(p,T)dp}{2.30 \cdot R \cdot T} \quad \dots(13)$$

with ΔH^0 and Δv^0 denoting the standard enthalpy and volume change, respectively, for the reaction considered (e.g. Kortuem (1966)).

We will use a highly simplified version of eq. (13) to derive approximate K values for state (p, T) from the reference state of most thermodynamic data compilations (1 atm, 298 K). The assumptions are :

(i) neglectation of pressure effects for reactions in or between condensed phases, that is setting

$$\Delta v^0(p,T) = 0 \quad \dots(14)$$

Although Δv^0 is expected to be small in such cases (data for dissolved actinide species seem to be completely lacking), assumption (14) might still lead to erroneous K values in the case of very high pressures (such as in granitic groundwaters at depth of 1000 m or more). Note that assumption (14) would be extremely poor if gases participate in the reaction, due their high compressibility.

(ii) constant reaction enthalpies for the temperature interval in question, i.e. assuming

$$\Delta H^0(p_0,T) = \Delta H^0(p_0,T_0) \quad \dots(15)$$

The reliability of this approximation, of course, generally decreases with increasing difference between T and T_0 . We will apply eq. (15) for a T_0 of 298 K within a T interval from 273 to 348 K (0 to 75 C). Indeed, the uncertainties associated with present data on dissolved actinide species do not justify further refinement.

Inserting eqs. (14) and (15) into (13) we derive

$$\log K(p,T) \approx \log K(p_0,T_0) + \frac{\Delta H^0(p_0,T_0)}{2.30 \cdot R} \left(\frac{1}{T_0} - \frac{1}{T} \right) \quad \dots(16)$$

II.2 Modelling of activity coefficients

The activity coefficients f_x for dissolved species in eq. (7) were modeled with Davies' approximation (see e.g. Stumm and Morgan (1970))

$$\log f_x = z_x^2 \cdot G(T,I) \quad \dots(17)$$

where

$$G(T,I) = -1.82E6 \cdot (\epsilon T)^{-3/2} \left\{ \frac{\sqrt{I}}{1 + \sqrt{I}} - 0.2 I \right\} \quad \dots(18)$$

with electric charge z_x for component or species X, ionic strength I and the dielectricity constant of pure water, ϵ , expressed by

$$\epsilon = 169.1 - 0.301 T \quad \dots(19)$$

The application range for eqs. (16) and (17) is limited to ionic strength interval 0 to 0.5.

Note that the activity coefficients of uncharged species are set to unity by eq. (18).

Values for G(T,I) are listed in Table B-1 for selected I values at 25 and 75 C.

Table B-1. G(T,I) for selected T and I.

<u>I</u>	<u>G(25 C, I)</u>	<u>G(75 C, I)</u>
0.	0.	0.
0.01	-0.045	-0.048
0.05	-0.086	-0.094
0.1	-0.110	-0.120
0.2	-0.1345	-0.1464